

# Accepted Manuscript

Discovery of novel polycyclic spiro-fused carbocyclicoxindole-based anticancer agents

Lidan Zhang, Wen Ren, Xiaoyan Wang, Jiaying Zhang, Jie Liu, Lifeng Zhao, Xia Zhang



PII: S0223-5234(16)31027-3

DOI: [10.1016/j.ejmech.2016.12.021](https://doi.org/10.1016/j.ejmech.2016.12.021)

Reference: EJMECH 9112

To appear in: *European Journal of Medicinal Chemistry*

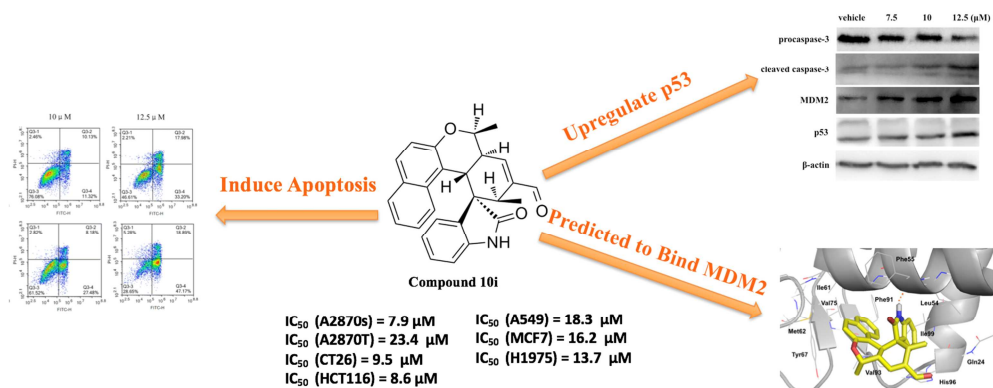
Received Date: 12 October 2016

Revised Date: 30 November 2016

Accepted Date: 9 December 2016

Please cite this article as: L. Zhang, W. Ren, X. Wang, J. Zhang, J. Liu, L. Zhao, X. Zhang, Discovery of novel polycyclic spiro-fused carbocyclicoxindole-based anticancer agents, *European Journal of Medicinal Chemistry* (2017), doi: 10.1016/j.ejmech.2016.12.021.

This is a PDF file of an unedited manuscript that has been accepted for publication. As a service to our customers we are providing this early version of the manuscript. The manuscript will undergo copyediting, typesetting, and review of the resulting proof before it is published in its final form. Please note that during the production process errors may be discovered which could affect the content, and all legal disclaimers that apply to the journal pertain.



# Discovery of novel polycyclic spiro-fused carbocyclooxindole-based anticancer agents

Lidan Zhang<sup>a,†</sup>, Wen Ren<sup>a,†</sup>, Xiaoyan Wang<sup>c</sup>, Jiaying Zhang<sup>d</sup>, Jie Liu<sup>a,\*</sup>, Lifeng Zhao<sup>b,\*</sup>, and Xia Zhang<sup>a,\*</sup>

<sup>a</sup> State Key Laboratory of Biotherapy and Cancer Center, West China Hospital, Sichuan University and Collaborative Innovation Center for Biotherapy, Chengdu 610041, China

<sup>b</sup> Chengdu University, Sichuan Industrial Institute of Antibiotics, Chengdu 610052, China

<sup>c</sup> Analytical & Testing Center, Sichuan University, Chengdu 610064, China

<sup>d</sup> Department of Ophthalmology, West China Hospital, Sichuan University, Chengdu 610041, China

\* Corresponding authors. E-mail addresses: liujie2011@scu.edu.cn (J. L.), lifengzhao@scu.edu.cn (L. Z.), zhang-xia@scu.edu.cn (X. Z.). Tel./fax: +86 28 85503817;

<sup>†</sup> These authors contributed equally.

## Abstract

A series of novel polycyclic spiro-fused carbocyclicoxindoles were synthesized and investigated for their *in vitro* antiproliferative activities against nine human cancer cell lines. Five compounds (**10i**, **10l**, **10n**, **10p**, and **10r**) demonstrated anticancer activities against A2780s cells with IC<sub>50</sub> values of less than 30  $\mu$ M. In particular, compound **10i** showed anticancer activities against seven cancer cell lines and stronger activities than cisplatin in A2780s, A2780T, CT26, and HCT116 cells. Further studies illustrated that compound **10i** arrested cell cycle in G1 phase and induced apoptosis of HCT116 cells. This compound also effectively increased the protein levels of cleaved caspase-3, p53, and MDM2. Molecular docking results revealed that compound **10i** could bind well to the p53-binding site on MDM2, indicating that it might work by blocking the MDM2-p53 interactions.

Keywords: polycyclic spiro-fused carbocyclicoxindoles; antiproliferative activity; p53 inducer; MDM2

## 1. Introduction

The p53 protein is a well-known tumor suppressor, which has a pivotal role in defending against tumor-associated DNA damage and regulating cell division.[1, 2] Under non-stressed conditions, p53 is maintained at low levels mainly by its negative regulator MDM2 protein through an auto-regulatory feedback loop.[3, 4] In response to cellular stresses including DNA damage and hyperproliferation, the protein levels of p53 are elevated, leading to cell cycle arrest, apoptosis, or senescence. The outcome of these events blocks cell proliferation or eliminates the cancer cells, and thus suppresses the development of cancer.[5]

Dysregulation of the p53 pathway, through mutations in *TP53* (the human gene that encodes p53) or inactivation of the components of the p53 pathway, is a common feature in human cancers.[6, 7] In about 50% of tumors, p53 is nonfunctional as a result of mutations in *TP53*. [7] The mutations in *TP53* inactivated p53 by altering the DNA-binding ability of p53 or changing the interactions of p53 with other proteins.[8] In cancers in which *TP53* is not mutated or deleted, the *mdm2* gene is usually found amplified or overexpressed to inhibit the function of p53.[9] As the primary negative regulator of p53, MDM2 deregulates the protein levels and the activity of p53 by promoting p53 degradation and blocking the binding of p53 to its targeted DNA.[10, 11] Thus, blockade of MDM2-p53 interaction may provide a novel method for the treatment of a broad spectrum of cancers.

The X-ray crystal structure of MDM2 with a transactivation domain peptide of p53 revealed that the p53 peptide binds to a hydrophobic cleft on MDM2.[12] Three p53 residues Phe19, Trp23, and Leu26, which are also involved in the transactivation, insert

deeply into the hydrophobic cavity on MDM2. Although targeting protein-protein interactions is usually viewed as a challenging task due to the typical flat binding sites, the existence of the well-defined p53-binding cavity on MDM2 suggests the possibility of the design of non-peptide inhibitors that bind to MDM2 and disrupt the MDM2-p53 interactions.[13]

In the past years, intensive efforts have been devoted to the search for efficient small-molecule inhibitors of the MDM2-p53 interactions.[1, 14, 15] A breakthrough in this field came from the discovery of the first series of small-molecule inhibitors Nutlins. The crystal structure of MDM2/Nutlin-2 complex illustrated that the inhibitor mimicked the structure of p53 peptide where the imidazoline scaffold of Nutlin-2 replaced the p53 peptide backbone and three substituents of Nutlin-2 positioned into the MDM2 pockets which were normally occupied by residues Phe19, Trp23, and Leu26 of p53. To date, ten small-molecule inhibitors have advanced into clinical trials as anticancer agents.[16-22] The representative structures of these inhibitors are shown in Figure 1. Among them, the spirooxindole-based inhibitor SAR405838 (MI-77301, compound 3, Figure 1) demonstrated a high binding affinity to MDM2 with a  $K_i$  value of 0.88nM.[20] Researchers found that the spirooxindole core structure of SAR405838 was essential for its binding affinity. The spirooxindole structure filled the Trp23 (p53) pocket on MDM2 and positioned other substituents to occupy the Phe19 (p53) and Leu26 (p53) pockets on MDM2.

To us, spirooxindole-based inhibitors such as SAR405838 represented a good opportunity for further investigations due to its high potency.[20, 23, 24] Based on the strategy of diversity-oriented synthesis, we developed a methodology for the efficient

construction of functionalized polycyclic spiro-fused carbocyclicoxindoles via an asymmetric organocatalytic quadruple-cascade reaction.[25] We postulated that by keeping the spirooxindole scaffold, the compounds produced by our methodology should retain the ability of mimicking the Trp23 residue of p53 and positioning other substituents to fill the pockets on MDM2. In addition, by using fused ring systems, we imposed structural constraints onto the ligands, which may reduce the entropic cost associated with the binding event. Herein, we report the anticancer activity of these polycyclic spiro-fused carbocyclicoxindoles and the preliminary mechanism studies of their anticancer effects.

## 2. Results and Discussion

### 2.1. Chemistry

The general synthetic route for the targeted compounds **10a-s** is outlined in Scheme 1. The easily accessible oxindole **6** was treated with salicylaldehyde **7** to obtain the key intermediate (*E*)-3-(2-hydroxybenzylidene)oxindole (**8**). The commercially available starting material crotonaldehyde (**9**) then reacted with **8** in the presence of  $\alpha,\alpha$ -*L*-diphenylprolinol trimethylsilyl ether and 2-(trifluoromethyl)benzoic acid in a quadruple-cascade manner to yield the polycyclic spiro-fused carbocyclicoxindole **10**. The reactions provided the targeted compounds in moderate to high yields (up to 90%). All the products were characterized by  $^1\text{H}$  NMR,  $^{13}\text{C}$  NMR, and ESI-MS analysis. The absolute configuration of compound **10i** was determined by X-ray crystallography. [26] Details of the discussions of this methodology was under separate cover.[25]

## 2.2. Biological evaluation

### 2.2.1. *In vitro* antiproliferative activity

The *in vitro* antiproliferative activities of the compounds **10a-s** were evaluated against multiple cell lines. The IC<sub>50</sub> (the concentration causing 50% inhibition of the tumor cell proliferation) values or percent inhibition (if the IC<sub>50</sub> of the corresponding compound was greater than 30  $\mu$ M) of the tested compounds against A2870s and A2870T cells were listed in Table 1. The IC<sub>50</sub> values of the tested compounds against H1299, BGC823, CT26, HCT116, A549, MCF7, and H1975 cells were listed in Table 2. Several compounds (compounds **10i**, **10l**, **10n**, **10p**, and **10r**) demonstrated moderate to favorable anti-proliferative activities against the A2870s cell line. Steric hindrance of the substituents on the carbocyclic group of the polycyclic portion decreased the activities of these compounds (compounds **10p** vs. **10a**, **10q-r**). The chlorine atom on the oxindole ring enhanced the compound potency (compounds **10l** vs. **10a**) in A2870s cells. Substituents on the distal phenyl ring of the polycyclic moiety did not affect the activity of the compounds dramatically in most cases (compounds **10b-h** vs. **10a**), with the bromide group enhancing the potency the most (**10f** vs. **10a**) in A2870s cells. The percent inhibition of compound **10o** (47.2%) against A2870s was much larger than that of compound **10a** (23.5%), indicating that the dihydro-pyridine substructure worked better than dihydro-pyran in A2870s cells. In addition, three compounds **10i**, **10n**, and **10p** showed activities of less than 30  $\mu$ M in multiple cell lines (Figure 2). Particularly, compound **10i** exhibited IC<sub>50</sub> values ranging from 7.9  $\mu$ M to 23.4  $\mu$ M against a broad spectrum of cancer cell lines including A2870s, A2870T, CT26, HCT116, A549, MCF7, and H1975. It also showed stronger activity than the positive control cisplatin in A2870s,



A2780T, CT26, and HCT116 cells. However, it did not inhibit the p53-deficient cell line H1299 with an  $IC_{50}$  value of less than 30  $\mu$ M, probably because compound **10i** worked by blocking the interactions between MDM2 and p53 and did not exert inhibitory effects on the p53-deficient cell lines. Interestingly, the compound **10n** showed antiproliferative activities against the the p53-deficient H1299 cell line, which indicated it might act through additional non-p53-related inhibitory mechanisms. Because of the strong activities of compound **10i** in multiple cell lines, the mechanisms of its antiproliferative effects were further investigated.

### 2.2.2. Cell cycle analysis

To elucidate the molecular mechanism by which compound **10i** suppressed proliferation of HCT116 cells, the effects of compound **10i** on cell cycle distribution were examined using flow cytometry. As shown in Figure 3, after exposure to compound **10i** at 7.5  $\mu$ M and 10  $\mu$ M for 24 h, significant accumulation of HCT116 cells in G1 phase, accompanied by a decrease of cells in S and G2 phases, was observed. The percentage of cells in G1 phase increased from 43.79% in the vehicle group to 46.10% and 75.18% in the groups treated with compound **10i** at concentrations of 7.5  $\mu$ M and 10  $\mu$ M, respectively. When treated with compound **10i** for 48 h, the HCT116 cells in G1 phase increased more dramatically. 82.32% of cells with treatment of compound **10i** at 10  $\mu$ M for 48 h accumulated in G1 phase. These results suggested that compound **10i** inhibited proliferation of HCT116 cells through inducing G1 phase arrest in a concentration- and time-dependent manner. Nutlin-3a, a selective inhibitor of MDM2-p53 interactions also

effectively arrested cell-cycle progression in HCT116 cells, but it induced both G1 and G2 arrest.[27]

### 2.2.3. Induced apoptosis by compound **10i**

The ability of compound **10i** to provoke apoptosis in HCT116 cells was then evaluated. After 24 h of treatment with compound **10i**, HCT116 cells displayed the morphological features of apoptotic cells including cell shrinkage (Figure 4A). The fluorescence microscopic examination of Hoechst 33342 staining cells further confirmed the apoptosis-inducing effects of compound **10i**. As shown in Figure 4B, nuclei condensation, cell-volume reduction, and nuclear fragmentation were observed in HCT116 cells after 24 h of treatment with compound **10i**. The flow cytometric analysis with PI-staining was then used to quantitatively assess the apoptotic effects of compound **10i**. As illustrated in Figure 5, the percentage of sub-G1 HCT116 cells in the **10i**-treated group increased in a concentration- and time-dependent manner. The apoptosis rate increased from 1.73% (control) to 3.18%, 15.92%, and 37.03% when cells were treated with compound **10i** at 7.5, 10 and 12.5  $\mu\text{M}$  for 24 h, respectively. The apoptosis augmented more dramatically with a rate up to 64.26% after 48 h of treatment with **10i** at 12.5  $\mu\text{M}$ . In addition, the flow cytometric analysis with Annexin V-FITC/PI fluorescence staining in HCT116 cells was used to further examine the apoptosis-inducing ability of compound **10i**. The experimental results indicated that the treatment with **10i** significantly induced concentration-dependent apoptosis in HCT116 cells (Figure 6). The percentage of apoptotic HCT116 cells treated with **10i** for 48 h increased from 6.27% to 66.06% when the concentration of **10i** increased from 7.5  $\mu\text{M}$  to 12.5  $\mu\text{M}$ . Similar results

were observed in HCT116 cells with treatment of **10i** for 24 h. These data confirmed that **10i** induced apoptosis of HCT116 cells in a concentration- and time-dependent manner.

#### 2.2.4. Upregulation of caspase-3, p53, and MDM2 by **10i**

The protein levels of procaspase-3, caspase-3, p53, and MDM2 in HCT116 cells treated with **10i** was monitored through western blot analysis. It is well known that caspase-3 plays an essential role in apoptosis.[28] The common events in apoptosis including cell shrinkage, chromatin condensation, and DNA fragmentation all require caspase-3. The results of the western blotting demonstrated that the treatment with **10i** for 24 h resulted in significant increase of the cleaved caspase-3 in a concentration-dependent manner (Figure 7). The activation of caspase-3 suggested that **10i** induced apoptosis in HCT116 cells through a cascade-dependent pathway. It was also observed that the treatment with **10i** enhanced the protein levels of p53 and MDM2. Notably, small-molecule inhibitors of MDM2-p53 interactions was expected to activate p53 and to increase the levels of p53 in cells with wild-type p53. Moreover, the activation of p53 by these inhibitors led to the induction of *mdm2*, a p53targeted gene, and as a result the protein levels of MDM2 were increased.[24] Thus, the phenomenon of enhanced levels of p53 and MDM2 by **10i** was consistent with that of the reported MDM2-p53 interaction inhibitors, suggesting that **10i** may work by blocking the MDM2-mediated p53 degradation and consequently lead to accumulation of p53 and transcriptional activation of the *mdm2* gene.[24, 29]

#### 2.2.5. Molecular docking analysis

The docking study of **10i** into the p53-binding site on MDM2 was then performed using GOLD software (version 5.0)[30]. The predicted binding mode of **10i** was illustrated in Figure 8. Similar to the reported spirooxindole-based MDM2-p53 interaction inhibitors, the NH on the oxindole group of **10i** exerted hydrogen-bonding interactions with the Leu54 backbone carbonyl group on MDM2. The oxindole group of **10i** extended into the Trp23 (p53) pocket on MDM2 and interacted with the hydrophobic sidechains of Leu54 and Ile99. In addition, the polycyclic portion of **10i** overlaid the Phe19 residue of p53 and formed intensive hydrophobic interactions with Ile61, Met62, Try67, Val75, Phe91, and Val93. Importantly, the distal phenyl group of the naphthalenyl moiety filled the Phe19 (p53) pocket. The other compounds without the naphthalene group presumably lacked the favorable hydrophobic interactions and shape complementarity, which may explain why those compounds have lower anticancer activities compared with **10i**.

### 3. Experimental Section

#### 3.1. Synthesis

##### 3.1.1. Materials and methods

$^1\text{H}$  NMR and  $^{13}\text{C}$  NMR spectra were recorded on a Bruker 400 MHz NMR spectrometer (Bruker BioSpin AG, Fällanden, Switzerland) at 400 and 100 MHz, respectively. Chemical shifts ( $\delta$ ) were reported in ppm with tetramethylsilane as an internal standard. ESI-HRMS spectra were recorded on a Waters SYNAPT G2.

Methanol was used to dissolve the sample. Melting points were recorded at SGW X-4

Melting point instrument (Shanghai precision & scientific instrument Co., Ltd, Shanghai,

China). All reagents and solvents were obtained from Alfa, Aldrich, and Energy Chemical and used without further purification. Column chromatography was performed on silica gel (300–400 mesh, Qingdao Marine Chemical Ltd, Qingdao, China).

### 3.1.2. General procedures for the preparation of substituted oxindole

Substituted isatin (10 mmol) was dissolved in hydrazine hydrate (98%, 10 mL, 32.5 mmol) and refluxed for 15-30 min (130 °C). The reaction mixture was then poured into cold water, extracted with ethyl acetate. The organic layer was then dried over sodium sulfate. Evaporation of the solvent and recrystallization from hexane/ethyl acetate provided the substituted oxindole.

### 3.1.3. General procedures for the preparation of substituted (*E*)-3-(2-hydroxybenzylidene)oxindole

The reaction mixture of the substituted oxindole (1 equiv), the substituted salicylaldehyde (1.2 equiv) and piperidine (0.1 equiv) in ethanol (1-2 mL/1 mmol) was stirred at 90 °C for 3-5 h. After the reaction mixture cooled down, the precipitate was filtered and washed with cold ethanol and diethyl ether, successively. Allowed to dry, the product was used in subsequent reaction without further purification.

### 3.1.4. General procedures for the preparation of polycyclic spiro-fused carbocyclicoxindoles

The crotonaldehyde (0.244 mmol) was added to a dry tube containing a suspension of (*E*)-3-(2-hydroxybenzylidene)oxindole (0.1 mmol),  $\alpha,\alpha$ -L-diphenylprolinol trimethylsilyl ether (0.02 mmol), 2-(trifluoromethyl)benzoic acid (0.06 mmol) and dry solvent (1 mL). The reaction mixture was stirred at 40 °C for 24 h and then heated up to

60 °C for 12 h. The reaction mixture was subjected to silica gel column chromatography to yield the corresponding product (petroleum ether/ ethyl acetate, 2/1, V/V).

### 3.1.5. Analytical and Spectral Characterization Data

#### **6,9-dimethyl-2'-oxo-6,6a,9,10a-tetrahydrospiro[benzo[c]chromene-10,3'-indoline]-8-carbaldehyde (10a)**

Light yellow solid; 80% yield; >99% ee; 8 : 1 dr; m.p. 125 °C -127 °C;  $[\alpha]_D^{22} = -49.8$  (c = 1.53 in CHCl<sub>3</sub>); HPLC (DAICEL CORPORATION AS-H), 2-propanol/n-hexane = 10/90, flow rate = 1.0 mL/min,  $\lambda = 254$  nm, retention time: 13.69 min (major) and 17.80 min (minor); <sup>1</sup>H NMR (400 MHz, CDCl<sub>3</sub>)  $\delta = 9.53$  (s, 1H), 8.86 (s, 1H), 7.28 (s, 1H), 7.13 (d,  $J = 7.2$  Hz, 1H), 6.98 (t,  $J = 7.2$  Hz, 2H), 6.90 (d,  $J = 7.6$  Hz, 1H), 6.86-6.73 (m, 2H), 6.41 (t,  $J = 7.6$  Hz, 1H), 5.99 (d,  $J = 7.6$  Hz, 1H), 4.40 (dq,  $J = 11.6, 6.0$  Hz, 1H), 3.67 (d,  $J = 10.4$  Hz, 1H), 3.21 (t,  $J = 10.4$  Hz, 1H), 2.81 (q,  $J = 6.4$  Hz, 1H), 1.60 (d,  $J = 6.0$  Hz, 3H), 1.19 (d,  $J = 6.8$  Hz, 3H). <sup>13</sup>C NMR (100 MHz, CDCl<sub>3</sub>)  $\delta = 193.0, 179.1, 154.6, 147.0, 143.7, 140.0, 131.0, 128.6, 127.9, 126.0, 125.8, 124.2, 122.1, 120.4, 117.2, 110.2, 77.7, 50.6, 44.0, 36.5, 34.8, 20.8, 18.9$ . HRMS (ESI-TOF) calcd for C<sub>23</sub>H<sub>21</sub>NO<sub>3</sub>  $[M+Na]^+ = 382.1414$ , Found 382.1415.

#### **4-fluoro-6,9-dimethyl-2'-oxo-6,6a,9,10a-tetrahydrospiro[benzo[c]chromene-10,3'-indoline]-8-carbaldehyde (10b)**

White solid; 75% yield; >99% ee; 6:1 dr; m.p. 59 °C-61 °C;  $[\alpha]_D^{22} = -50.0$  (c = 0.074 in CHCl<sub>3</sub>); HPLC (DAICEL CORPORATION AS-H), 2-propanol/n-hexane = 15/85, flow rate = 1.0 mL/min,  $\lambda = 254$  nm, retention time: 11.99 min (major) and 14.07 min (minor); <sup>1</sup>H NMR (400 MHz, CDCl<sub>3</sub>)  $\delta = 9.54$  (s, 1H), 7.95 (s, 1H), 7.32 (t,  $J = 7.6$  Hz, 1H), 7.17

(d,  $J = 7.6$  Hz, 1H), 7.07-6.94 (m, 2H), 6.88-6.77 (m, 2H), 6.37 (td,  $J = 8.0, 5.2$  Hz, 1H), 5.79 (d,  $J = 8.0$  Hz, 1H), 4.48 (dq,  $J = 12.0, 6.0$  Hz, 1H), 3.69 (d,  $J = 10.4$  Hz, 1H), 3.24 (t,  $J = 10.8$  Hz, 1H), 2.84 (q,  $J = 6.8$  Hz, 1H), 1.68 (d,  $J = 6.0$  Hz, 3H), 1.21 (d,  $J = 7.2$  Hz, 3H).  $^{13}\text{C}$  NMR (100 MHz,  $\text{CDCl}_3$ )  $\delta = 192.9, 179.3, 146.3, 143.8, 142.7, 140.0, 130.8, 128.7, 128.3, 125.9, 122.2, 119.9, 119.3, 114.8, 114.6, 110.4, 78.3, 50.7, 43.9, 36.5, 34.8, 20.7, 18.9$ . HRMS (ESI-TOF) calcd for  $\text{C}_{23}\text{H}_{20}\text{FNO}_3$   $[\text{M}+\text{Na}]^+ = 400.1319$ , Found 400.1325.

**3-methoxy-6,9-dimethyl-2'-oxo-6,6a,9,10a-tetrahydrospiro[benzo[c]chromene-10,3'-indoline]-8-carbaldehyde (10c)**

Light yellow solid; 65% yield; >99% ee; 5:1 dr; m.p. 70 °C-72 °C;  $[\alpha]_{\text{D}}^{22} = -42.3$  ( $c = 0.40$  in  $\text{CHCl}_3$ ); HPLC (DAICEL CORPORATION AS-H), 2-propanol/*n*-hexane = 10/90, flow rate = 1.0 mL/min,  $\lambda = 254$  nm, retention time: 17.63 min (major) and 21.38 min (minor);  $^1\text{H}$  NMR (400 MHz,  $\text{CDCl}_3$ )  $\delta = 9.53$  (s, 1H), 7.31 (t,  $J = 7.6$  Hz, 1H), 7.19 (d,  $J = 7.6$  Hz, 1H), 7.03 (t,  $J = 7.6$  Hz, 1H), 6.96 (d,  $J = 7.6$  Hz, 1H), 6.83 (d,  $J = 2.4$  Hz, 1H), 6.38 (d,  $J = 2.4$  Hz, 1H), 6.00 (dd,  $J = 8.8, 2.4$  Hz, 1H), 5.88 (d,  $J = 8.8$  Hz, 1H), 4.38 (dq,  $J = 12.2, 6.0$  Hz, 1H), 3.65 (s, 4H), 3.23 (t,  $J = 10.4$  Hz, 1H), 2.81 (q,  $J = 6.8$  Hz, 1H), 1.62 (d,  $J = 6.0$  Hz, 3H), 1.19 (d,  $J = 4.8$  Hz, 3H).  $^{13}\text{C}$  NMR (100 MHz,  $\text{CDCl}_3$ )  $\delta = 193.0, 179.4, 159.5, 155.7, 146.9, 143.9, 140.1, 131.1, 128.6, 126.0, 124.9, 122.1, 117.5, 110.3, 106.0, 102.8, 77.6, 55.2, 50.9, 44.0, 36.1, 34.7, 20.7, 19.0$ . HRMS (ESI-TOF) calcd for  $\text{C}_{24}\text{H}_{23}\text{NO}_4$   $[\text{M}+\text{Na}]^+ = 412.1519$ , Found 412.1533.

**2-fluoro-6,9-dimethyl-2'-oxo-6,6a,9,10a-tetrahydrospiro[benzo[c]chromene-10,3'-indoline]-8-carbaldehyde (10d)**

White solid; 72% yield; 98% ee; 7:1 dr; m.p. 61 °C-63 °C;  $[\alpha]_D^{22} = -24.5$  ( $c = 0.33$  in  $\text{CHCl}_3$ ); HPLC (DAICEL CORPORATION AS-H), 2-propanol/*n*-hexane = 10/90, flow rate = 1.0 mL/min,  $\lambda = 254$  nm, retention time: 15.51 min (major) and 18.96 min (minor);  $^1\text{H}$  NMR (400 MHz,  $\text{CDCl}_3$ )  $\delta = 9.53$  (s, 1H), 8.00 (s, 1H), 7.34 (t,  $J = 7.6$  Hz, 1H), 7.18 (d,  $J = 7.6$  Hz, 1H), 7.08-6.97 (m, 2H), 6.81 (d,  $J = 2.4$  Hz, 1H), 6.76-6.66 (m, 2H), 5.73 (dd,  $J = 10.0, 2.4$  Hz, 1H), 4.37 (dq,  $J = 12.0, 6.0$  Hz, 1H), 3.64 (d,  $J = 10.4$  Hz, 1H), 3.18 (t,  $J = 10.8$  Hz, 1H), 2.83 (q,  $J = 6.8$  Hz, 1H), 1.59 (d,  $J = 6.0$  Hz, 3H), 1.21 (d,  $J = 6.8$  Hz, 3H).  $^{13}\text{C}$  NMR (100 MHz,  $\text{CDCl}_3$ )  $\delta = 192.9, 179.2, 150.6, 146.6, 143.7, 140.1, 130.4, 129.0, 127.1, 127.1, 126.0, 122.3, 117.9, 117.8, 114.3, 114.1, 111.5, 111.3, 110.6, 77.5, 50.6, 43.8, 36.5, 34.8, 20.7, 18.8$ . HRMS (ESI-TOF) calcd for  $\text{C}_{23}\text{H}_{20}\text{FNO}_3$   $[\text{M}+\text{Na}]^+ = 400.1319$ , Found 400.1329.

**2-chloro-6,9-dimethyl-2'-oxo-6,6a,9,10a-tetrahydrospiro[benzo[c]chromene-10,3'-indoline]-8-carbaldehyde (10e)**

White solid; 65% yield; 98% ee; 6:1 dr; m.p. 54 °C-56 °C;  $[\alpha]_D^{22} = -61.3$  ( $c = 0.266$  in  $\text{CHCl}_3$ ); HPLC (DAICEL CORPORATION AS-H), 2-propanol/*n*-hexane = 5/95, flow rate = 1.0 mL/min,  $\lambda = 254$  nm, retention time: 31.17 min (major) and 39.05 min (minor);  $^1\text{H}$  NMR (400 MHz,  $\text{CDCl}_3$ )  $\delta = 9.53$  (s, 1H), 7.36 (t,  $J = 7.6$  Hz, 1H), 7.18 (d,  $J = 7.6$  Hz, 1H), 7.10-6.99 (m, 2H), 6.95 (dd,  $J = 8.4, 2.0$  Hz, 1H), 6.82 (d,  $J = 2.4$  Hz, 1H), 6.72 (d,  $J = 8.4$  Hz, 1H), 5.94 (d,  $J = 1.2$  Hz, 1H), 4.38 (dq,  $J = 12.0, 6.0$  Hz, 1H), 3.63 (d,  $J = 10.4$  Hz, 1H), 3.21 (t,  $J = 10.4$  Hz, 1H), 2.84 (q,  $J = 6.8$  Hz, 1H), 1.60 (d,  $J = 6.0$  Hz, 3H),



1.21 (d,  $J = 6.8$  Hz, 3H).  $^{13}\text{C}$  NMR (100 MHz,  $\text{CDCl}_3$ )  $\delta$  192.9, 178.8, 153.3, 146.3, 143.8, 140.1, 130.4, 129.0, 127.8, 126.9, 126.0, 125.0, 124.7, 122.3, 118.3, 110.4, 77.7, 50.5, 43.5, 36.5, 34.7, 20.6, 18.9. HRMS (ESI-TOF) calcd for  $\text{C}_{23}\text{H}_{20}\text{ClNO}_3$   $[\text{M}+\text{Na}]^+ = 416.1024$ , Found 416.1033.

**2-bromo-6,9-dimethyl-2'-oxo-6,6a,9,10a-tetrahydrospiro[benzo[c]chromene-10,3'-indoline]-8-carbaldehyde (10f)**

White solid; 70% yield; 98% ee; 7:1 dr; m.p. 94 °C-96 °C;  $[\alpha]_{\text{D}}^{22} = -72.6$  ( $c = 1.15$  in  $\text{CHCl}_3$ ); HPLC (DAICEL CORPORATION AS-H), 2-propanol/*n*-hexane = 5/95, flow rate = 1.0 mL/min,  $\lambda = 254$  nm, retention time: 32.81 min (major) and 37.87 min (minor);  $^1\text{H}$  NMR (400 MHz,  $\text{CDCl}_3$ )  $\delta$  = 9.54 (s, 1H), 7.70 (s, 1H), 7.37 (t,  $J = 7.6$  Hz, 1H), 7.19 (d,  $J = 7.6$  Hz, 1H), 7.12-7.00 (m, 3H), 6.82 (d,  $J = 2.4$  Hz, 1H), 6.67 (d,  $J = 8.8$  Hz, 1H), 6.08 (d,  $J = 1.2$  Hz, 1H), 4.38 (dq,  $J = 12.0, 6.0$  Hz, 1H), 3.64 (d,  $J = 10.4$  Hz, 1H), 3.21 (t,  $J = 11.2$  Hz, 1H), 2.85 (q,  $J = 6.8$  Hz, 1H), 1.61 (d,  $J = 6.0$  Hz, 3H), 1.22 (d,  $J = 7.2$  Hz, 3H).  $^{13}\text{C}$  NMR (100 MHz,  $\text{CDCl}_3$ )  $\delta$  = 192.9, 178.9, 153.8, 146.3, 143.8, 140.0, 130.7, 130.4, 129.0, 127.7, 127.3, 126.0, 122.4, 118.7, 112.4, 110.4, 77.7, 50.6, 43.4, 36.5, 34.6, 20.6, 18.9. HRMS (ESI-TOF) calcd for  $\text{C}_{23}\text{H}_{20}\text{BrNO}_3$   $[\text{M}+\text{Na}]^+ = 460.0519$ , Found 460.0525.

**2-nitro-6,9-dimethyl-2'-oxo-6,6a,9,10a-tetrahydrospiro[benzo[c]chromene-10,3'-indoline]-8-carbaldehyde (10g)**

White solid; 35% yield; 98% ee; 4:1 dr; m.p. 104 °C-106 °C;  $[\alpha]_{\text{D}}^{22} = -87.1$  ( $c = 0.31$  in  $\text{CHCl}_3$ ); HPLC (DAICEL CORPORATION AD-H), 2-propanol/*n*-hexane = 20/80, flow

rate = 1.0 mL/min,  $\lambda$  = 254 nm, retention time: 11.05 min (major) and 17.27 min (minor);  $^1\text{H}$  NMR (400 MHz,  $\text{CDCl}_3$ )  $\delta$  = 9.58 (s, 1H), 7.93 (dd,  $J$  = 9.2, 2.4 Hz, 1H), 7.78 (s, 1H), 7.43 (t,  $J$  = 7.6 Hz, 1H), 7.22 (d,  $J$  = 7.6 Hz, 1H), 7.17-7.07 (m, 2H), 7.04 (d,  $J$  = 1.6 Hz, 1H), 6.86 (d,  $J$  = 8.8 Hz, 2H), 4.53 (dq,  $J$  = 12.4, 6.0 Hz, 1H), 3.70 (d,  $J$  = 10.4 Hz, 1H), 3.31 (t,  $J$  = 10.8 Hz, 1H), 2.92 (q,  $J$  = 6.8 Hz, 1H), 1.71 (d,  $J$  = 6.0 Hz, 3H), 1.26 (d,  $J$  = 7.2 Hz, 3H).  $^{13}\text{C}$  NMR (100 MHz,  $\text{CDCl}_3$ )  $\delta$  = 192.7, 178.7, 160.4, 145.0, 144.3, 140.9, 140.3, 129.9, 129.4, 125.8, 125.0, 124.3, 122.5, 121.7, 117.3, 111.1, 79.0, 50.5, 42.7, 36.6, 34.4, 20.4, 19.1. HRMS (ESI-TOF) calcd for  $\text{C}_{23}\text{H}_{20}\text{N}_2\text{O}_5$   $[\text{M}+\text{Na}]^+$  = 427.1264, Found 427.1277.

**2,6,9-trimethyl-2'-oxo-6,6a,9,10a-tetrahydrospiro[benzo[c]chromene-10,3'-indoline]-8-carbaldehyde (10h)**

White solid; 75% yield; >99% ee; 5:1 dr; m.p. 75 °C-77 °C;  $[\alpha]_{\text{D}}^{22}$  = -44.3 ( $c$  = 0.33 in  $\text{CHCl}_3$ ); HPLC (DAICEL CORPORATION AS-H), 2-propanol/*n*-hexane = 10/90, flow rate = 1.0 mL/min,  $\lambda$  = 254 nm, retention time: 10.61 min (major) and 12.35 min (minor);  $^1\text{H}$  NMR (400 MHz,  $\text{CDCl}_3$ )  $\delta$  = 9.54 (s, 1H), 7.71 (s, 1H), 7.32 (t,  $J$  = 7.6 Hz, 1H), 7.18 (d,  $J$  = 7.6 Hz, 1H), 7.07-6.94 (m, 2H), 6.82 (dd,  $J$  = 14.8, 5.2 Hz, 2H), 6.69 (d,  $J$  = 8.0 Hz, 1H), 5.78 (s, 1H), 4.37 (dq,  $J$  = 12.0, 6.0 Hz, 1H), 3.66 (d,  $J$  = 10.4 Hz, 1H), 3.20 (t,  $J$  = 10.4 Hz, 1H), 2.83 (q,  $J$  = 7.2 Hz, 1H), 1.84 (s, 3H), 1.60 (d,  $J$  = 6.0 Hz, 3H), 1.22 (d,  $J$  = 7.2 Hz, 3H).  $^{13}\text{C}$  NMR (100 MHz,  $\text{CDCl}_3$ )  $\delta$  = 193.1, 179.3, 152.3, 147.2, 143.7, 140.2, 131.1, 129.3, 128.6, 128.3, 126.2, 125.3, 125.1, 122.1, 116.8, 110.0, 50.7, 44.1, 36.5, 34.7, 20.7, 20.7, 18.9. HRMS (ESI-TOF) calcd for  $\text{C}_{24}\text{H}_{23}\text{NO}_3$   $[\text{M}+\text{Na}]^+$  = 396.1570, Found 396.1575.

**2,5-dimethyl-2'-oxo-2,4a,5,12c-tetrahydrospiro[dibenzo[c,f]chromene-1,3'-indoline]-3-carbaldehyde (10i)**

White solid; 65% yield; >99% ee; 1:4 dr; m.p. 60 °C-62 °C;  $[\alpha]_D^{22} = 55.6$  (c = 0.16 in CHCl<sub>3</sub>); HPLC (DAICEL CORPORATION AD-H, 2-propanol/*n*-hexane = 20/80, flow rate = 1.0 mL/min,  $\lambda$  = 254 nm, retention time: 8.20 min (major) and 9.28 min (minor); <sup>1</sup>H NMR (400 MHz, CDCl<sub>3</sub>)  $\delta$  = 9.71 (s, 1H), 7.60-7.50 (m, 2H), 7.33 (t, *J* = 7.2 Hz, 1H), 7.15 (t, *J* = 7.6 Hz, 1H), 7.05 (dd, *J* = 16.0, 8.4 Hz, 4H), 6.72 (d, *J* = 7.8 Hz, 1H), 6.62 (q, *J* = 8.4 Hz, 2H), 4.92 (dd, *J* = 6.4, 4.0 Hz, 1H), 3.66 (dt, *J* = 12.0, 4.4 Hz, 1H), 3.50-3.44 (m, 1H), 3.17 (d, *J* = 6.8 Hz, 1H), 1.33 (d, *J* = 6.8 Hz, 4H), 0.98 (d, *J* = 7.2 Hz, 3H). <sup>13</sup>C NMR (100 MHz, CDCl<sub>3</sub>)  $\delta$  = 191.1, 178.6, 152.3, 151.9, 142.2, 141.8, 134.8, 133.0, 129.3, 129.2, 128.5, 128.0, 124.3, 123.8, 123.2, 122.8, 122.5, 120.1, 114.5, 109.9, 70.7, 56.4, 43.3, 42.5, 41.4, 22.7, 14.1. HRMS (ESI-TOF) calcd for C<sub>27</sub>H<sub>23</sub>NO<sub>3</sub> [M+Na]<sup>+</sup> = 432.1570, Found 432.1585.

**5',6,9-trimethyl-2'-oxo-6,6a,9,10a-tetrahydrospiro[benzo[c]chromene-10,3'-indoline]-8-carbaldehyde (10j)**

White solid; 67% yield; 98% ee; 6:1 dr; m.p. 122 °C-124 °C;  $[\alpha]_D^{22} = -56.4$  (c = 0.69 in CHCl<sub>3</sub>); HPLC (DAICEL CORPORATION AS-H), 2-propanol/*n*-hexane = 5/95, flow rate = 1.0 mL/min,  $\lambda$  = 254 nm, retention time: 20.85 min (major) and 26.50 min (minor); <sup>1</sup>H NMR (400 MHz, CDCl<sub>3</sub>)  $\delta$  = 9.53 (s, 1H), 8.34 (s, 1H), 7.08 (d, *J* = 8.0 Hz, 1H), 7.03-6.95 (m, 2H), 6.82 (t, *J* = 8.0 Hz, 3H), 6.45 (t, *J* = 7.6 Hz, 1H), 6.03 (d, *J* = 7.6 Hz, 1H), 4.40 (dq, *J* = 12.0, 6.0 Hz, 1H), 3.65 (d, *J* = 10.4 Hz, 1H), 3.20 (t, *J* = 10.4 Hz, 1H), 2.80

(q,  $J = 6.8$  Hz, 1H), 2.28 (s, 3H), 1.61 (d,  $J = 6.0$  Hz, 3H), 1.20 (d,  $J = 7.2$  Hz, 3H).  $^{13}\text{C}$  NMR (100 MHz,  $\text{CDCl}_3$ )  $\delta = 193.1, 179.9, 154.6, 147.0, 143.9, 137.8, 131.4, 131.0, 128.9, 127.8, 126.6, 126.0, 124.5, 120.5, 117.1, 110.2, 77.7, 50.8, 44.1, 36.5, 34.8, 21.3, 20.8, 19.0$ . HRMS (ESI-TOF) calcd for  $\text{C}_{24}\text{H}_{23}\text{NO}_3$   $[\text{M}+\text{Na}]^+ = 396.1570$ , Found 396.1581.

**5'-fluoro-6,9-dimethyl-2'-oxo-6,6a,9,10a-tetrahydrospiro[benzo[c]chromene-10,3'-indoline]-8-carbaldehyde (10k)**

White solid; 80% yield; 96% ee; 6:1 dr; m.p.  $109\text{ }^\circ\text{C}$ - $111\text{ }^\circ\text{C}$ ;  $[\alpha]_{\text{D}}^{22} = -43.7$  ( $c = 0.35$  in  $\text{CHCl}_3$ ); HPLC (DAICEL CORPORATION AS-H), 2-propanol/ $n$ -hexane = 10/90, flow rate = 1.0 mL/min,  $\lambda = 254$  nm, retention time: 13.96 min (major) and 20.39 min (minor);  $^1\text{H}$  NMR (400 MHz,  $\text{CDCl}_3$ )  $\delta = 9.54$  (s, 1H), 7.96 (s, 1H), 7.02 (dt,  $J = 8.8, 4.4$  Hz, 2H), 6.96-6.87 (m, 2H), 6.88-6.76 (m, 2H), 6.48 (t,  $J = 7.6$  Hz, 1H), 6.00 (d,  $J = 7.6$  Hz, 1H), 4.40 (dq,  $J = 12.0, 6.0$  Hz, 1H), 3.63 (d,  $J = 10.4$  Hz, 1H), 3.19 (t,  $J = 10.8$  Hz, 1H), 2.84 (q,  $J = 6.8$  Hz, 1H), 1.61 (d,  $J = 6.0$  Hz, 3H), 1.21 (d,  $J = 6.4$  Hz, 3H).  $^{13}\text{C}$  NMR (100 MHz,  $\text{CDCl}_3$ )  $\delta = 192.8, 179.2, 159.8, 154.6, 146.8, 143.4, 136.1, 132.7, 128.0, 125.5, 124.0, 120.5, 117.3, 115.0, 113.8, 110.8, 92.8, 77.6, 51.2, 44.1, 36.6, 34.8, 20.8, 18.8$ . HRMS (ESI-TOF) calcd for  $\text{C}_{23}\text{H}_{20}\text{FNO}_3$   $[\text{M}+\text{Na}]^+ = 400.1319$ , Found 400.1320.

**6'-chloro-6,9-dimethyl-2'-oxo-6,6a,9,10a-tetrahydrospiro[benzo[c]chromene-10,3'-indoline]-8-carbaldehyde (10l)**

Light yellow solid; 90% yield; >99% ee; 7:1 dr; m.p.  $139\text{ }^\circ\text{C}$ - $141\text{ }^\circ\text{C}$ ;  $[\alpha]_{\text{D}}^{22} = -29.0$  ( $c = 1.12$  in  $\text{CHCl}_3$ ); HPLC (DAICEL CORPORATION AS-H), 2-propanol/ $n$ -hexane =

10/90, flow rate = 1.0 mL/min,  $\lambda$  = 254 nm, retention time: 13.96 min (major) and 19.58 min (minor);  $^1\text{H}$  NMR (400 MHz,  $\text{CDCl}_3$ )  $\delta$  = 9.53 (s, 1H), 8.99 (s, 1H), 7.09-6.92 (m, 4H), 6.84 (dd,  $J$  = 12.4, 5.2 Hz, 2H), 6.48 (t,  $J$  = 7.6 Hz, 1H), 5.99 (d,  $J$  = 7.6 Hz, 1H), 4.40 (dq,  $J$  = 12.0, 6.0 Hz, 1H), 3.65 (d,  $J$  = 10.4 Hz, 1H), 3.18 (t,  $J$  = 10.4 Hz, 1H), 2.80 (q,  $J$  = 6.8 Hz, 1H), 1.63 (d,  $J$  = 6.0 Hz, 3H), 1.17 (d,  $J$  = 6.8 Hz, 3H).  $^{13}\text{C}$  NMR (100 MHz,  $\text{CDCl}_3$ )  $\delta$  = 193.0, 180.1, 154.6, 147.0, 143.5, 141.5, 134.3, 129.4, 128.1, 126.6, 125.6, 124.0, 122.1, 120.6, 117.3, 111.3, 77.7, 50.7, 44.1, 36.4, 34.8, 20.8, 18.9. HRMS (ESI-TOF) calcd for  $\text{C}_{23}\text{H}_{20}\text{ClNO}_3$   $[\text{M}+\text{Na}]^+$  = 416.1024, Found 416.1023.

**1',6,9-trimethyl-2'-oxo-6,6a,9,10a-tetrahydrospiro[benzo[c]chromene-10,3'-indoline]-8-carbaldehyde (10m)**

White solid; 31% yield; 94% ee; 10:1 dr; m.p. 62 °C-64 °C;  $[\alpha]_{\text{D}}^{22}$  = -52.0 (c = 0.10 in  $\text{CHCl}_3$ ); HPLC (DAICEL CORPORATION AS-H), 2-propanol/*n*-hexane = 10/90, flow rate = 1.0 mL/min,  $\lambda$  = 254 nm, retention time: 17.80 min (major) and 22.07 min (minor);  $^1\text{H}$  NMR (400 MHz,  $\text{CDCl}_3$ )  $\delta$  = 9.53 (s, 1H), 7.41 (t,  $J$  = 7.6 Hz, 1H), 7.28 (s, 1H), 7.08 (t,  $J$  = 7.6 Hz, 1H), 6.99 (dd,  $J$  = 7.2, 4.0 Hz, 2H), 6.79 (d,  $J$  = 8.8 Hz, 2H), 6.41 (t,  $J$  = 7.6 Hz, 1H), 5.86 (d,  $J$  = 7.6 Hz, 1H), 5.02-4.87 (m, 1H), 3.79-3.69 (m, 2H), 3.19 (s, 3H), 2.69 (dd,  $J$  = 14.0, 6.8 Hz, 1H), 1.42 (d,  $J$  = 6.4 Hz, 3H), 1.24 (d,  $J$  = 7.2 Hz, 3H).  $^{13}\text{C}$  NMR (100 MHz,  $\text{CDCl}_3$ )  $\delta$  = 192.8, 177.5, 154.9, 146.9, 143.4, 143.2, 130.7, 128.7, 127.9, 125.6, 125.6, 124.2, 122.1, 120.1, 117.2, 108.8, 77.3, 77.2, 77.0, 76.7, 73.5, 58.5, 50.4, 41.4, 34.7, 19.1, 18.4, 17.8. HRMS (ESI-TOF) calcd for  $\text{C}_{24}\text{H}_{23}\text{NO}_3$   $[\text{M}+\text{Na}]^+$  = 396.1570, Found 396.1573.

**6,9-dimethyl-2'-oxo-1'-phenyl-6,6a,9,10a-tetrahydrospiro[benzo[c]chromene-10,3'-indoline]-8-carbaldehyde (10n)**

White solid; 45% yield; 92% ee; 12:1 dr; m.p. 72 °C-74 °C;  $[\alpha]_D^{22} = -25.6$  (c = 0.50 in CHCl<sub>3</sub>); HPLC (DAICEL CORPORATION AS-H, 2-propanol/*n*-hexane = 3/97, flow rate = 1.0 mL/min,  $\lambda$  = 254 nm, retention time: 32.66 min (major) and 37.55 min (minor); <sup>1</sup>H NMR (400 MHz, CDCl<sub>3</sub>)  $\delta$  = 7.49 (t, *J* = 7.6 Hz, 2H), 7.39 (d, *J* = 7.6 Hz, 1H), 7.34 (t, *J* = 6.8 Hz, 4H), 7.10 (t, *J* = 7.2 Hz, 1H), 7.03 (t, *J* = 7.2 Hz, 1H), 6.95 (d, *J* = 7.6 Hz, 1H), 6.83 (d, *J* = 7.6 Hz, 1H), 6.79 (d, *J* = 2.0 Hz, 1H), 6.49 (t, *J* = 7.2 Hz, 1H), 6.14 (d, *J* = 7.6 Hz, 1H), 5.05-4.87 (m, 1H), 3.86-3.74 (m, 2H), 2.91 (q, *J* = 6.8 Hz, 1H), 1.44 (d, *J* = 6.4 Hz, 3H), 1.31 (d, *J* = 7.2 Hz, 3H). <sup>13</sup>C NMR (100 MHz, CDCl<sub>3</sub>)  $\delta$  = 192.8, 177.0, 155.1, 146.8, 143.3, 134.2, 130.4, 129.6, 128.6, 128.2, 128.0, 126.7, 125.9, 125.8, 124.2, 122.6, 120.1, 117.3, 110.1, 73.6, 50.4, 41.5, 34.9, 31.1, 19.0, 17.8. HRMS (ESI-TOF) calcd for C<sub>29</sub>H<sub>25</sub>NO<sub>3</sub> [M+Na]<sup>+</sup> = 458.1727, Found 458.1728.

**6',9'-dimethyl-2-oxo-6',6a',9',10a'-tetrahydro-5'H-spiro[indoline-3,10'-phenanthridine]-8'-carbaldehyde (10o)**

Light orange solid; 83% yield; >99% ee; 2.5:1 dr; m.p. 121 °C-123 °C;  $[\alpha]_D^{22} = -88.8$  (c = 0.55 in CHCl<sub>3</sub>); HPLC (DAICEL CORPORATION AD-H), 2-propanol/*n*-hexane = 20/80, flow rate = 1.0 mL/min,  $\lambda$  = 254 nm, retention time: 19.96 min (major) and 17.34 min (minor); <sup>1</sup>H NMR (400 MHz, CDCl<sub>3</sub>)  $\delta$  = 9.54 (s, 1H), 8.37 (s, 1H), 7.24 (d, *J* = 7.6 Hz, 1H), 7.12 (d, *J* = 7.2 Hz, 1H), 7.00-6.89 (m, 3H), 6.86 (t, *J* = 7.6 Hz, 1H), 6.48 (d, *J* = 7.6 Hz, 1H), 6.21 (t, *J* = 7.6 Hz, 1H), 5.94 (d, *J* = 7.6 Hz, 1H), 3.65-3.46 (m, 2H), 2.92 (t, *J* = 10.0 Hz, 1H), 2.80 (q, *J* = 6.8 Hz, 1H), 1.47 (d, *J* = 6.0 Hz, 3H), 1.18 (d, *J* = 6.8 Hz,

3H).  $^{13}\text{C}$  NMR (100 MHz,  $\text{CDCl}_3$ )  $\delta$  = 193.4, 180.2, 149.0, 144.5, 143.3, 140.1, 131.5, 128.3, 127.2, 125.8, 124.1, 123.0, 121.9, 117.0, 113.5, 110.3, 53.8, 51.0, 43.3, 37.8, 35.0, 22.4, 18.9. HRMS (ESI-TOF) calcd for  $\text{C}_{23}\text{H}_{22}\text{N}_2\text{O}_2$   $[\text{M}+\text{Na}]^+ = 381.1573$ , Found 381.1584.

**2'-oxo-6,6a,9,10a-tetrahydrospiro[benzo[c]chromene-10,3'-indoline]-8-carbaldehyde (10p)**

Light yellow solid; 55% yield; 64% ee; 1:2.5 dr; m.p. 98 °C-100 °C;  $[\alpha]_{\text{D}}^{22} = 14.6$  ( $c = 0.35$  in  $\text{CHCl}_3$ ); HPLC (DAICEL CORPORATION AS-H), 2-propanol/*n*-hexane = 20/80, flow rate = 1.0 mL/min,  $\lambda = 254$  nm, retention time: 16.65 min (major) and 23.05 min (minor);  $^1\text{H}$  NMR (400 MHz,  $\text{CDCl}_3$ )  $\delta$  = 9.57 (s, 1H), 8.28 (s, 1H), 7.32 (t,  $J = 7.6$  Hz, 1H), 7.22 (d,  $J = 7.6$  Hz, 1H), 7.12 (t,  $J = 7.6$  Hz, 1H), 7.06-6.93 (m, 2H), 6.82 (s, 1H), 6.78 (d,  $J = 8.0$  Hz, 1H), 6.44 (t,  $J = 7.2$  Hz, 1H), 6.18 (d,  $J = 8.0$  Hz, 1H), 4.68 (dd,  $J = 10.0, 4.0$  Hz, 1H), 4.18-4.07 (m, 1H), 3.95 (t,  $J = 11.2$  Hz, 1H), 3.51 (d,  $J = 10.4$  Hz, 1H), 2.78 (d,  $J = 18.8$  Hz, 1H), 2.65 (d,  $J = 18.8$  Hz, 1H).  $^{13}\text{C}$  NMR (100 MHz,  $\text{CDCl}_3$ )  $\delta$  = 192.7, 179.7, 154.8, 146.3, 139.9, 138.3, 134.5, 128.7, 128.4, 125.4, 123.6, 122.9, 122.6, 120.4, 117.1, 110.4, 70.2, 47.5, 41.4, 35.6, 34.4. HRMS (ESI-TOF) calcd for  $\text{C}_{21}\text{H}_{17}\text{NO}_3$   $[\text{M}+\text{Na}]^+ = 354.1101$ , Found 354.1103.

**6,9-diethyl-2'-oxo-6,6a,9,10a-tetrahydrospiro[benzo[c]chromene-10,3'-indoline]-8-carbaldehyde (10q)**

Yellow solid; 60% yield; >99% ee; 3:1 dr; m.p. 53 °C-55 °C;  $[\alpha]_{\text{D}}^{22} = -86.3$  ( $c = 0.23$  in  $\text{CHCl}_3$ ); HPLC (DAICEL CORPORATION AD-H, 2-propanol/*n*-hexane = 5/95, flow

rate = 1.0 mL/min,  $\lambda$  = 220 nm, retention time: 22.05 min (major) and 30.51 min (minor);  $^1\text{H}$  NMR (400 MHz,  $\text{CDCl}_3$ )  $\delta$  = 9.58 (s, 1H), 8.03 (s, 1H), 7.31 (t,  $J$  = 7.6 Hz, 1H), 7.21 (d,  $J$  = 7.6 Hz, 1H), 7.00 (dd,  $J$  = 16.4, 7.6 Hz, 3H), 6.85 (dd,  $J$  = 13.6, 5.2 Hz, 2H), 6.46 (t,  $J$  = 7.6 Hz, 1H), 5.99 (d,  $J$  = 7.6 Hz, 1H), 4.33-4.17 (m, 1H), 3.70 (d,  $J$  = 10.4 Hz, 1H), 3.19 (t,  $J$  = 10.0 Hz, 1H), 2.74 (t,  $J$  = 5.8 Hz, 1H), 2.12-2.03 (m, 1H), 1.93-1.84 (m, 1H), 1.78 (dt,  $J$  = 14.4, 7.2 Hz, 1H), 1.54-1.45 (m, 1H), 1.17 (t,  $J$  = 7.2 Hz, 3H), 0.73 (t,  $J$  = 7.2 Hz, 3H).  $^{13}\text{C}$  NMR (100 MHz,  $\text{CDCl}_3$ )  $\delta$  = 193.1, 179.5, 154.9, 147.6, 142.6, 140.1, 131.0, 128.6, 127.8, 126.7, 125.7, 123.9, 122.3, 120.5, 117.2, 110.3, 82.1, 51.2, 42.2, 40.8, 37.6, 27.3, 26.4, 13.1, 9.2. HRMS (ESI-TOF) calcd for  $\text{C}_{25}\text{H}_{25}\text{NO}_3$   $[\text{M}+\text{Na}]^+$  = 410.1727, Found 410.1725.

**2'-oxo-6,9-dipropyl-6,6a,9,10a-tetrahydrospiro[benzo[c]chromene-10,3'-indoline]-8-carbaldehyde (10r)**

Yellow solid; 78% yield; >99% ee; 4:1 dr; m.p. 129 °C-131 °C;  $[\alpha]_{\text{D}}^{22}$  = -84.7 ( $c$  = 0.66 in  $\text{CHCl}_3$ ); HPLC (DAICEL CORPORATION AD-H), 2-propanol/*n*-hexane = 7/93, flow rate = 1.0 mL/min,  $\lambda$  = 220 nm, retention time: 13.68 min (major) and 21.51 min (minor);  $^1\text{H}$  NMR (400 MHz,  $\text{CDCl}_3$ )  $\delta$  = 9.57 (s, 1H), 8.60 (s, 1H), 7.30 (td,  $J$  = 7.6, 0.8 Hz, 1H), 7.19 (d,  $J$  = 7.2 Hz, 1H), 7.06-6.93 (m, 3H), 6.83 (t,  $J$  = 5.6 Hz, 2H), 6.46 (t,  $J$  = 7.6 Hz, 1H), 5.98 (d,  $J$  = 7.6 Hz, 1H), 4.39- 4.19 (m, 1H), 3.69 (d,  $J$  = 10.4 Hz, 1H), 3.16 (td,  $J$  = 10.8, 1.6 Hz, 1H), 2.76 (t,  $J$  = 5.6 Hz, 1H), 1.99-1.88 (m, 1H), 1.79-1.72 (m, 3H), 1.66-1.55 (m, 1H), 1.46-1.34 (m, 1H), 1.23-1.15 (m, 1H), 1.05 (t,  $J$  = 7.2 Hz, 4H), 0.96-0.79 (m, 3H), 0.75 (t,  $J$  = 7.2 Hz, 3H).  $^{13}\text{C}$  NMR (100 MHz,  $\text{CDCl}_3$ )  $\delta$  = 193.1, 180.3, 154.8, 147.3, 143.1, 140.2, 131.0, 128.6, 127.7, 126.8, 125.4, 124.0, 122.3, 120.6, 117.3, 110.6,



80.9, 51.2, 42.7, 39.9, 37.6, 36.6, 36.0, 22.1, 18.2, 14.2, 14.1. HRMS (ESI-TOF) calcd for  $C_{27}H_{29}NO_3$   $[M+Na]^+ = 438.2040$ , Found 438.2042.

**6,6,9-trimethyl-2'-oxo-6,6a,9,10a-tetrahydrospiro[benzo[c]chromene-10,3'-indoline]-8-carbaldehyde (10s)**

White solid; 50% yield; 97% ee; 5:1 dr; m.p. 65 °C-67 °C;  $[\alpha]_D^{22} = -59.2$  (c = 0.31 in  $CHCl_3$ ); HPLC (DAICEL CORPORATION AS-H, 2-propanol/*n*-hexane = 10/90, flow rate = 1.0 mL/min,  $\lambda = 254$  nm, retention time: 12.13 min (major) and 14.02 min (minor);  $^1H$  NMR (400 MHz,  $CDCl_3$ )  $\delta = 9.54$  (s, 1H), 8.19 (s, 1H), 7.29 (t,  $J = 7.6$  Hz, 1H), 7.19 (d,  $J = 7.2$  Hz, 1H), 7.06-6.91 (m, 3H), 6.81 (dd,  $J = 14.4, 5.2$  Hz, 2H), 6.49 (t,  $J = 7.6$  Hz, 1H), 6.06 (d,  $J = 7.6$  Hz, 1H), 3.65 (d,  $J = 10.8$  Hz, 1H), 3.25 (d,  $J = 10.8$  Hz, 1H), 2.81 (q,  $J = 6.8$  Hz, 1H), 1.61 (s, 3H), 1.43 (s, 3H), 1.23 (d,  $J = 7.2$  Hz, 3H).  $^{13}C$  NMR (100 MHz,  $CDCl_3$ )  $\delta = 192.9, 179.7, 154.5, 147.7, 143.3, 140.1, 131.1, 128.5, 128.0, 127.7, 125.8, 123.8, 122.1, 120.8, 117.7, 110.3, 79.6, 50.7, 48.2, 34.5, 33.0, 28.8, 24.5, 18.8$ . HRMS (ESI-TOF) calcd for  $C_{24}H_{23}NO_3$   $[M+Na]^+ = 396.1570$ , Found 396.1576.

### 3.2. Biological evaluation

#### 3.2.1. Antiproliferative activity assay

The MTT method was used to evaluate the antiproliferative activities of the synthesized polycyclic spiro-fused carbocyclooxindole derivatives. Targeted cancer cell lines ( $3 \times 10^3$ /well) were seeded in 96-well plates and cultured for 24 h, followed by the treatment with compounds **10a-s** (final concentrations of 30, 15, 7.5, 3.8, 1.9, and 0.9  $\mu M$ ) for 48 h. A solution of 20  $\mu L$  5 mg/mL MTT was added per well and incubated for

another 2-4 h at 37 °C, and then the supernatant fluid was removed and 150  $\mu$ L DMSO were added per well for 15-20 min. The absorptions (OD) were measured at 570 nm using Spectra MAX M5 microplate spectrophotometer (Molecular Devices, LLC, Sunnyvale, CA, USA). The effect of compounds on cancer cell viability was expressed by IC<sub>50</sub> of each cell line. Each assay was carried out at least three times.

### 3.2.2. Cell-cycle distribution and apoptosis detection analysis by flow cytometry

Cell cycle distributions in cells were determined through PI staining. HCT116 Cells were seeded in 6-well plates at the density of  $1 \times 10^5$  cells/well and cultured for 24 h, followed by the treatment of compound **10i** with concentration of 0, 7.5, 10, and 12.5  $\mu$ M for another 24 h and 48 h. Next, cells were harvested. Sediments were re-suspended in 1 mL hypotonic fluorochrome solution (50  $\mu$ g/mL PI in 0.1% sodium citrate plus 0.1% Triton X-100), and then analyzed by flow cytometer (Novo Cyte, ACEA bioscience, USA). Cell cycle distribution was then estimated with software NovoExpress 1.1.2.

The extent of apoptosis induced by compound **10i** was quantitatively measured using PI staining and Annexin V-FITC/PI staining assays. Following the instructions of the PI and Annexin V-FITC/PI detection kits, HCT116 cells ( $1 \times 10^6$  cells/mL) were seeded in 6-well plates for 24 h and then were treated with compound **10i** (0, 7.5, 10, and 12.5  $\mu$ M) for another 24 h and 48 h. Cells were then collected and washed twice with PBS and stained with 5  $\mu$ L PI solution or 5  $\mu$ L of Annexin V-FITC and 1  $\mu$ L of PI (100  $\mu$ g/mL) in 1 $\times$ binding buffer (10 mM HEPES, pH 7.4, 140 mM NaOH, 2.5 mM CaCl<sub>2</sub>) at room temperature for 30 minutes in the dark. Apoptotic cells were quantified using flow cytometry. The percentages of early apoptotic (Annexin V-FITC positive, PI negative) and late apoptotic (double positive of Annexin V-FITC and PI) cells were determined

using software NovoExpress 1.1.2.

### 3.2.3. Hoechst staining

HCT116 cells ( $1 \times 10^5$ /well) were seeded in 6-well plates and cultured for 24 h, followed by the treatment of **10i** with different final concentrations (0, 7.5, 10, and 12.5  $\mu$ M) for another 24 h. After rinsing with phosphate buffered saline (PBS), the cells were fixed using 75% of ethanol. The morphological change of cells was examined by inverted microscope. After that, the cells were stained with Hoechst 33342 (2  $\mu$ g/mL, in PBS) and analysed under fluorescence microscope (Zeiss, Axiovert 200, Germany) to identify the apoptotic cells.

### 3.2.4 Western blot analysis

After treatment with **10i**, HCT116 cells were lysed in radio-immunoprecipitation assay (RIPA) lysis buffer (Beyotime Institute of Biotechnology, Nantong, Jiangsu Province, China) with 1% cocktail (Sigma-Aldrich, St. Louis, MO, USA) on ice. Next, lysates were centrifuged at 13000 g for 20 min at 4 °C. The supernatant was harvested and the protein concentration was measured by the BCA method. Equal amounts of total proteins were subjected to SDS-PAGE and transferred onto polyvinylidene fluoride (PVDF) membranes (Millipore, Bedford, MA, USA). The membranes were incubated with each antibody and detected by immunoblot analysis. All antibodies were purchased from Cell Signaling Technology, Inc. (Boston, MA, USA) and diluted in accordance with the manufacturer's instruction. After incubation with the specific primary and secondary antibodies, the protein bands were visualized using an enhanced chemiluminescent substrate to horseradish peroxidase (Amersham, Piscataway, NJ).

### 3.3. Molecular docking analysis

Predicted bound configurations of compound **10i** were obtained using GOLD software (version 5.0)[30] with 4OAS.pdb[21] representing the human MDM2 structure. The preparation of the protein structure including adding hydrogen atoms and removing water molecules was conducted using the docking wizard in GOLD. The three-dimensional structure of compound **10i** was constructed and minimized using ChemBio3D ultra (version 12.0, CambridgeSoft Corporation, USA). CHEMPLP was selected as the scoring function for pose prediction. The docking pose of compound **10i** was visualized using PyMOL (version 0.99rc6, Schrödinger Inc., New York, NY, USA).

## 4. Concluding Remarks

In conclusion, we synthesized a novel series of polycyclic spiro-fused carbocyclooxindoles and evaluated their anticancer activities against multiple cancer cell lines. Five compounds (**10i**, **10l**, **10n**, **10p**, and **10r**) exhibited  $IC_{50}$  values of less than 30  $\mu$ M in A2780s cells. The most potent compound **10i** in A2780s cells ( $IC_{50} = 7.9 \mu$ M) also displayed inhibitory activities against a panel of other cancer cell lines including A2870T, CT26, HCT116, A549, MCF7, and H1975. Notably, **10i** outperformed cisplatin in A2870s, A2870T, CT26, and HCT116 cells. The Hoechst 33342 staining assays and the flow cytometric analyses with PI staining and Annexin V-FITC/PI staining indicated that **10i** induced apoptosis. The western blotting results illustrated that the treatment of **10i** led to upregulation of cleaved caspase-3 in HCT116 cells and suggested that **10i** induce apoptosis through a cascade-dependent pathway. **10i** also enhanced the protein levels of p53 and MDM2, indicating it blocked MDM2-mediated p53 degradation. The molecular docking study of **10i** into the p53-binding site on MDM2 further supported that

**10i** might work as an MDM2-p53 interaction inhibitor. However, the exact molecular mechanism of the upregulation of p53 and MDM2 requires additional investigation.

#### Acknowledgement

We appreciate the funding support from the National Natural Science Foundation of China (Nos. 81573290 and 81202403). We also thank Sichuan University Analytical & Testing Center for NMR analysis.

## References

- [1] L.T. Vassilev, B.T. Vu, B. Graves, D. Carvajal, F. Podlaski, Z. Filipovic, N. Kong, U. Kammlott, C. Lukacs, C. Klein, N. Fotouhi, E.A. Liu, In vivo activation of the p53 pathway by small-molecule antagonists of MDM2, *Science*, 303 (2004) 844-848.
- [2] D.W. Meek, Tumour suppression by p53: a role for the DNA damage response?, *Nat. Rev. Cancer.*, 9 (2009) 714-723.
- [3] K.H. Khoo, C.S. Verma, D.P. Lane, Drugging the p53 pathway: understanding the route to clinical efficacy (vol 13, pg 217, 2014), *Nat. Rev. Drug. Discov.*, 13 (2014).
- [4] J.D. Oliner, K.W. Kinzler, P.S. Meltzer, D.L. George, B. Vogelstein, Amplification of a Gene Encoding a P53-Associated Protein in Human Sarcomas, *Nature*, 358 (1992) 80-83.
- [5] T. Riley, E. Sontag, P. Chen, A. Levine, Transcriptional control of human p53-regulated genes, *Nat. Rev. Mol. Cell. Bio.*, 9 (2008) 402-412.
- [6] P.A.J. Muller, K.H. Vousden, p53 mutations in cancer, *Nat. Cell. Biol.*, 15 (2013) 2-8.
- [7] B. Vogelstein, D. Lane, A.J. Levine, Surfing the p53 network, *Nature*, 408 (2000) 307-310.
- [8] S.K. Thukral, Y. Lu, G.C. Blain, T.S. Harvey, V.L. Jacobsen, Discrimination of DNA-Binding Sites by Mutant P53 Proteins, *Mol. Cell. Biol.*, 15 (1995) 5196-5202.
- [9] D.A. Freedman, L. Wu, A.J. Levine, Functions of the MDM2 oncoprotein, *Cell. Mol. Life. Sci.*, 55 (1999) 96-107.
- [10] X.W. Wu, J.H. Bayle, D. Olson, A.J. Levine, The P53 Mdm-2 Autoregulatory Feedback Loop, *Gene. Dev.*, 7 (1993) 1126-1132.
- [11] T. Juven-Gershon, M. Oren, Mdm2: The ups and downs, *Mol. Med.*, 5 (1999) 71-83.
- [12] P.H. Kussie, S. Gorina, V. Marechal, B. Elenbaas, J. Moreau, A.J. Levine, N.P. Pavletich, Structure of the MDM2 oncoprotein bound to the p53 tumor suppressor transactivation domain, *Science*, 274 (1996) 948-953.
- [13] D. Gonzalez-Ruiz, H. Gohlke, Targeting protein-protein interactions with small molecules: Challenges and perspectives for computational binding epitope detection and ligand finding, *Curr. Med. Chem.*, 13 (2006) 2607-2625.
- [14] Y. Rew, D.Q. Sun, F.G.L. De Turiso, M.D. Bartberger, H.P. Beck, J. Canon, A. Chen, D. Chow, J. Deignan, B.M. Fox, D. Gustin, X. Huang, M. Jiang, X.Y. Jiao, L.X. Jin, F. Kayser, D.J. Kopecky, Y.H. Li, M.C. Lo, A.M. Long, K. Michelsen, J.D. Oliner, T. Osgood, M. Ragains, A.Y. Saiki, S. Schneider, M. Toteva, P. Yakowec, X.L. Yan, Q.P. Ye, D.Y. Yu, X.N. Zhao, J. Zhou, J.C. Medina, S.H. Olson, Structure-Based Design of Novel Inhibitors of the MDM2-p53 Interaction, *J. Med. Chem.*, 55 (2012) 4936-4954.
- [15] B.L. Grasberger, T.B. Lu, C. Schubert, D.J. Parks, T.E. Carver, H.K. Koblish, M.D. Cummings, L.V. LaFrance, K.L. Milkiewicz, R.R. Calvo, D. Maguire, J. Lattanze, C.F. Franks, S.Y. Zhao, K. Ramachandren, G.R. Bylebyl, M. Zhang, C.L. Manthey, E.C. Petrella, M.W. Pantoliano, I.C. Deckman, J.C. Spurlino, A.C. Maroney, B.E. Tomczuk, C.J. Molloy, R.F. Bone, Discovery and cocrystal structure of benzodiazepinedione HDM2 antagonists that activate p53 in cells, *J. Med. Chem.*, 48 (2005) 909-912.
- [16] P. Holzer, K. Masuya, P. Furet, J. Kallen, T. Valat-Stachyra, S. Ferretti, J. Berghausen, M. Bouisset-Leonard, N. Buschmann, C. Pissot-Soldermann, C. Rynn, S. Ruetz, S. Stutz, P. Chene, S. Jeay, F. Gessier, Discovery of a Dihydroisoquinolinone

Derivative (NVP-CGM097): A Highly Potent and Selective MDM2 Inhibitor Undergoing Phase 1 Clinical Trials in p53wt Tumors, *J. Med. Chem.*, 58 (2015) 6348-6358.

[17] Y.J. Zhao, A. Aguilar, D. Bernard, S.M. Wang, Small-Molecule Inhibitors of the MDM2-p53 Protein-Protein Interaction (MDM2 Inhibitors) in Clinical Trials for Cancer Treatment, *J. Med. Chem.*, 58 (2015) 1038-1052.

[18] B. Vu, P. Wovkulich, G. Pizzolato, A. Lovey, Q.J. Ding, N. Jiang, J.J. Liu, C.L. Zhao, K. Glenn, Y. Wen, C. Tovar, K. Packman, L. Vassilev, B. Graves, Discovery of RG7112: A Small-Molecule MDM2 Inhibitor in Clinical Development, *Acc. Med. Chem. Lett.*, 4 (2013) 466-469.

[19] Q.J. Ding, Z.M. Zhang, J.J. Liu, N. Jiang, J. Zhang, T.M. Ross, X.J. Chu, D. Bartkovitz, F. Podlaski, C. Janson, C. Tovar, Z.M. Filipovic, B. Higgins, K. Glenn, K. Packman, L.T. Vassilev, B. Graves, Discovery of RG7388, a Potent and Selective p53-MDM2 Inhibitor in Clinical Development, *J. Med. Chem.*, 56 (2013) 5979-5983.

[20] S.M. Wang, W. Sun, Y.J. Zhao, D. McEachern, I. Meaux, C. Barriere, J.A. Stuckey, J.L. Meagher, L.C. Bai, L. Liu, C.G. Hoffman-Luca, J.F. Lu, S. Shangary, S.H. Yu, D. Bernard, A. Aguilar, O. Dos-Santos, L. Besret, S. Guerif, P. Pannier, D. Gorge-Bernat, L. Debussche, SAR405838: An Optimized Inhibitor of MDM2-p53 Interaction That Induces Complete and Durable Tumor Regression, *Cancer. Res.*, 74 (2014) 5855-5865.

[21] D.Q. Sun, Z.H. Li, Y. Rew, M. Gribble, M.D. Bartberger, H.P. Beck, J. Canon, A. Chen, X.Q. Chen, D. Chow, J. Deignan, J. Duquette, J. Eksterowicz, B. Fisher, B.M. Fox, J.S. Fu, A.Z. Gonzalez, F.G.L. De Turiso, J.B. Houze, X. Huang, M. Jiang, L.X. Jin, F. Kayser, J.W. Liu, M.C. Lo, A.M. Long, B. Lucas, L.R. McGee, J. McIntosh, J. Mihalic, J.D. Oliner, T. Osgood, M.L. Peterson, P. Roveto, A.Y. Saiki, P. Shaffer, M. Toteva, Y.C. Wang, Y.C. Wang, S. Wortman, P. Yakowec, X.L. Yan, Q.P. Ye, D.Y. Yu, M. Yu, X.N. Zhao, J. Zhou, J. Zhu, S.H. Olson, J.C. Medina, Discovery of AMG 232, a Potent, Selective, and Orally Bioavailable MDM2-p53 Inhibitor in Clinical Development, *J. Med. Chem.*, 57 (2014) 1454-1472.

[22] <https://clinicaltrials.gov/ct2/results?term=MDM2>. Accessed Sep 27, 2016.

[23] K. Ding, Y. Lu, Z. Nikolovska-Coleska, S. Qiu, Y.S. Ding, W. Gao, J. Stuckey, K. Krajewski, P.P. Roller, Y. Tomita, D.A. Parrish, J.R. Deschamps, S.M. Wang, Structure-based design of potent non-peptide MDM2 inhibitors, *J. Am. Chem. Soc.*, 127 (2005) 10130-10131.

[24] K. Ding, Y.P. Lu, Z. Nikolovska-Coleska, G.P. Wang, S. Qiu, S. Shangary, W. Gao, D.G. Qin, J. Stuckey, K. Krajewski, P.P. Roller, S.M. Wang, Structure-based design of spiro-oxindoles as potent, specific small-molecule inhibitors of the MDM2-p53 interaction, *J. Med. Chem.*, 49 (2006) 3432-3435.

[25] W Ren, X-Y Wang, J-J Li, M Tian, J Liu, L Ouyang, J-H Wang, Efficient Construction of Biologically Important Functionalized Polycyclic Spiro-fused Carbocyclicoxindoles via an Asymmetric Organocatalytic Quadruple-Cascade Reaction, *RSC Adv.*, in-press.

[26] Crystallographic data of **10i** reported in this manuscript have been deposited with Cambridge Crystallographic Data Centre as supplementary publication no. CCDC-1448116. Copies of the data can be obtained free of charge via <http://www.ccdc.cam.ac.uk/deposit> (or from the Cambridge Crystallographic Data Centre, 12, Union Road, Cambridge, CB2 1EZ, UK. fax: +44 1223 336033; or [deposit@ccdc.cam.ac.uk](mailto:deposit@ccdc.cam.ac.uk)).

- [27] C. Tovar, J. Rosinski, Z. Filipovic, B. Higgins, K. Kolinsky, H. Hilton, X.L. Zhao, B.T. Vu, W.G. Qing, K. Packman, O. Myklebost, D.C. Heimbrosk, L.T. Vassilev, Small-molecule MDM2 antagonists reveal aberrant p53 signaling in cancer: Implications for therapy, *P. Natl. Acad. Sci. USA.*, 103 (2006) 1888-1893.
- [28] A.G. Porter, R.U. Janicke, Emerging roles of caspase-3 in apoptosis, *Cell. Death. Differ.*, 6 (1999) 99-104.
- [29] S. Shangary, D.G. Qin, D. McEachern, M.L. Liu, R.S. Miller, S. Qiu, Z. Nikolovska-Coleska, K. Ding, G.P. Wang, J.Y. Chen, D. Bernard, J. Zhang, Y.P. Lu, Q.Y. Gu, R.B. Shah, K.J. Pienta, X.L. Ling, S.M. Kang, M. Guo, Y. Sun, D.J. Yang, S.M. Wang, Temporal activation of p53 by a specific MDM2 inhibitor is selectively toxic to tumors and leads to complete tumor growth inhibition, *P. Natl. Acad. Sci. USA.*, 105 (2008) 3933-3938.
- [30] G. Jones, P. Willett, R.C. Glen, A.R. Leach, R. Taylor, Development and validation of a genetic algorithm for flexible docking, *J. Mol. Biol.*, 267 (1997) 727-748.



# Figure Captions:

Figure 1. Representative MDM2 inhibitors in clinical development.

Figure 2. Antiproliferative activities of the compounds **10i**, **10n**, **10p**, and cisplatin against H1299, BGC823, CT26, HCT116, A549, MCF7, and H1975 cells *in vitro*.

Figure 3. Effects of compound **10i** on cell cycle distribution: DNA fluorescence histograms of PI-stained HCT116 cells. Cells were treated with 7.5  $\mu$ M, 10  $\mu$ M, 12.5  $\mu$ M for 24 h and 48 h.

Figure 4. Effects of compound **10i** on cell morphology: (A) bright-field microscopy images and (B) fluorescence microscopic appearance of Hoechst 33342 staining nuclei of HCT116 cells, after incubation with compound **10i** for 24 h at varying concentrations: 7.5  $\mu$ M, 10  $\mu$ M, 12.5  $\mu$ M. Apoptosis cells were observed in treated cells containing condensed and fragmented fluorescent nuclei.

Figure 5. Compound **10i** induces apoptosis in HCT116 cells. Flow cytometric analysis of PI-stained HCT116 cell lines after treatment with 7.5  $\mu$ M, 10  $\mu$ M, 12.5  $\mu$ M for 24 h and 48 h.

Figure 6. Flow cytometric analysis of cells stained with Annexin V-FITC/PI after treatment with various concentrations (7.5  $\mu$ M, 10  $\mu$ M, 12.5  $\mu$ M) of compound **10i** for 24 h and 48 h.

Figure 7. The effects of compound **10i** on levels of procaspase-3, cleaved caspase-3, MDM2, and P53 determined by western blot.  $\beta$ -actin levels served as loading controls.

Figure 8. Predicted binding configuration of compound **10i** (non-polar hydrogen atoms undisplayed) into the p53-binding site on MDM2 (4OAS.pdb[21]).

Scheme 1. Synthetic route to spirooxindole derivatives **10a-s**.

ACCEPTED MANUSCRIPT

Figures:

Figure 1. Representative MDM2 inhibitors in clinical development

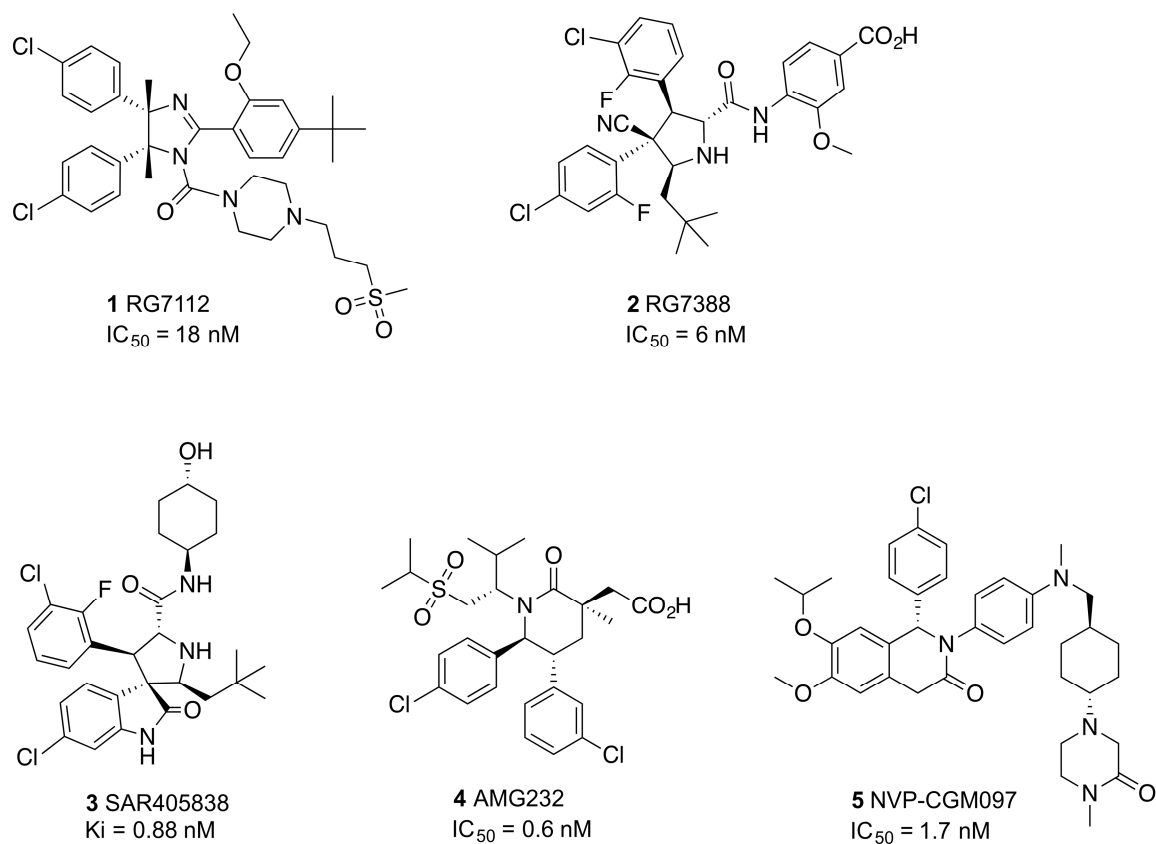


Figure 2. Antiproliferative activities of the compounds **10i**, **10n**, **10p**, and cisplatin against H1299, BGC823, CT26, HCT116, A549, MCF7, and H1975 cells *in vitro*.

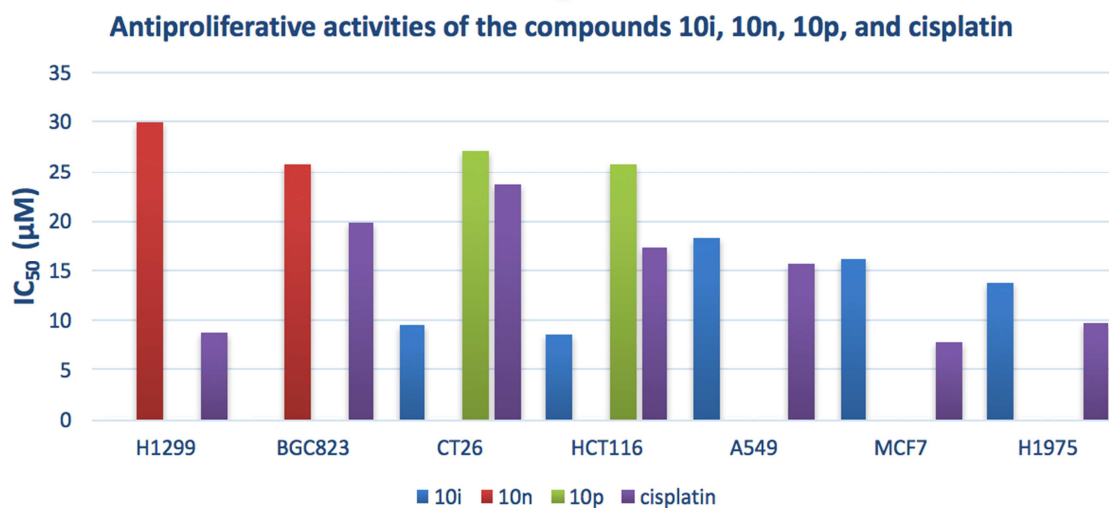


Figure 3. Effects of compound **10i** on cell cycle distribution: DNA fluorescence histograms of PI-stained HCT116 cells. Cells were treated with compound **10i** at concentrations of 7.5  $\mu$ M and 10  $\mu$ M for 24 h and 48 h, respectively.

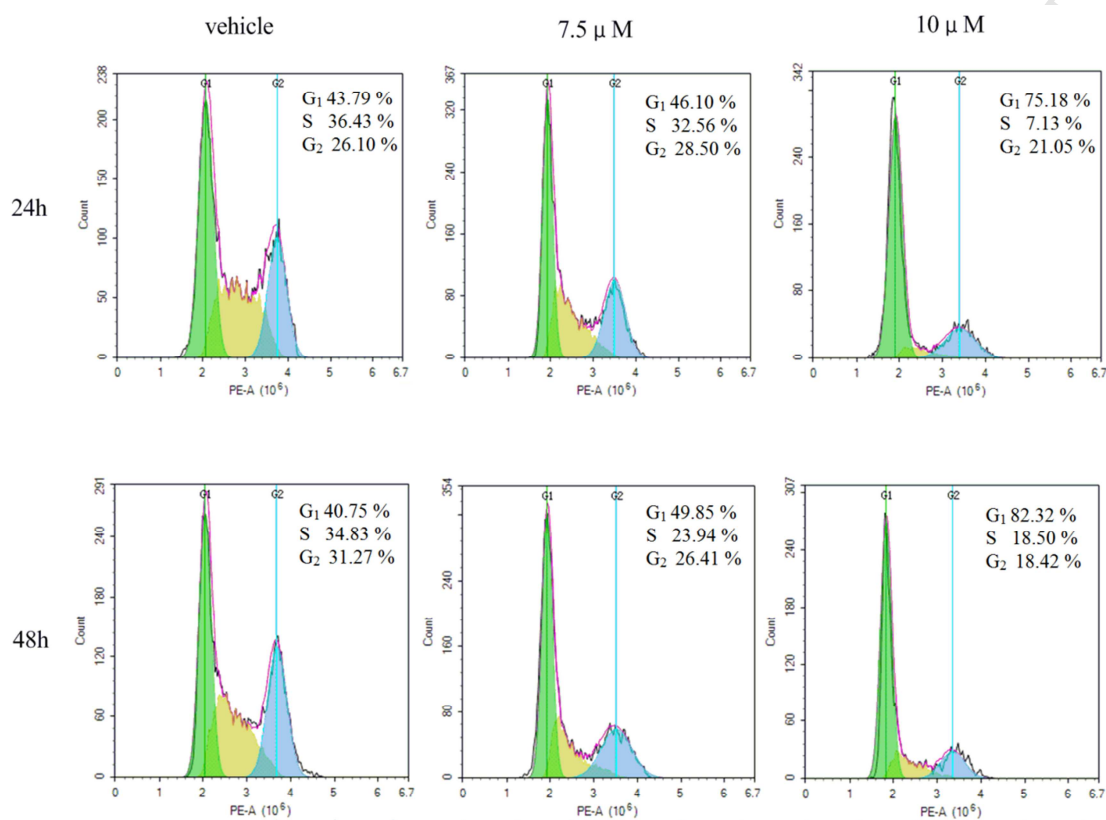


Figure 4. Effects of compound **10i** on cell morphology: (A) bright-field microscopy images and (B) fluorescence microscopic appearance of Hoechst 33342 staining nuclei of HCT116 cells, after incubation with compound **10i** for 24 h at concentrations of 7.5  $\mu$ M, 10  $\mu$ M, and 12.5  $\mu$ M.

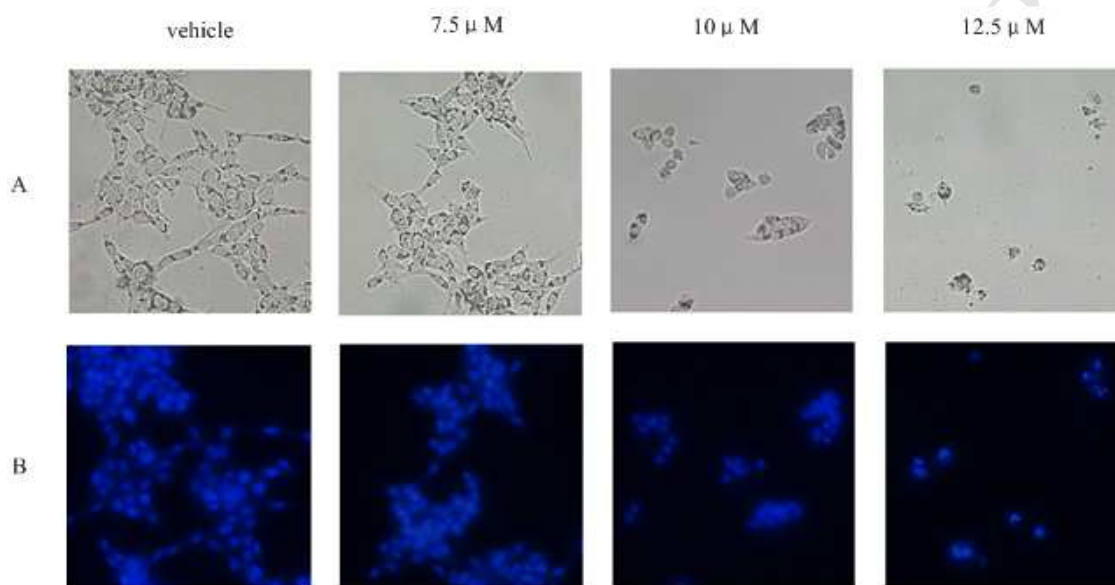


Figure 5. Compound **10i** induces apoptosis in HCT116 cells. Flow cytometric analysis of PI-stained HCT116 cell lines after treatment with compound **10i** at concentrations of 7.5  $\mu$ M, 10  $\mu$ M, and 12.5  $\mu$ M for 24 h and 48 h.

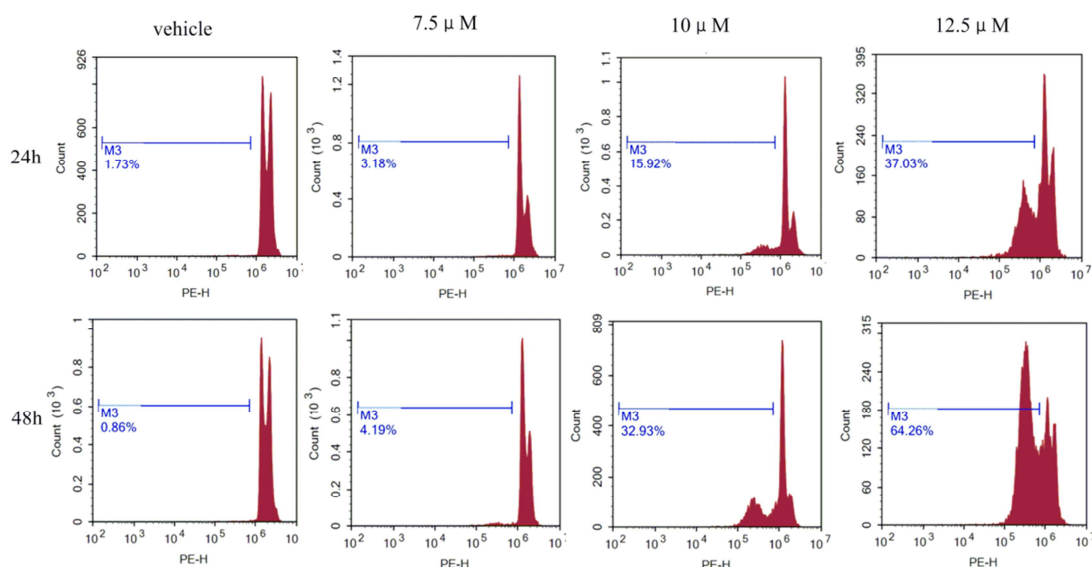


Figure 6. Flow cytometric analysis of cells stained with Annexin V-FITC/PI after treatment with compound **10i** at concentrations of 7.5  $\mu$ M, 10  $\mu$ M, and 12.5  $\mu$ M for 24 h and 48 h, respectively.

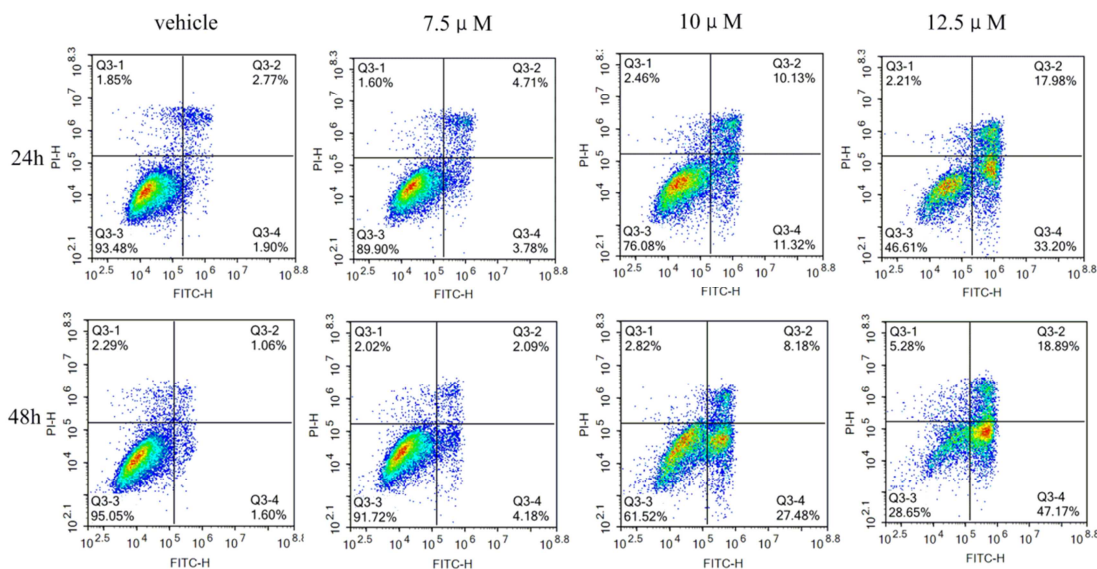




Figure 7. The effects of compound **10i** on levels of procaspase-3, cleaved caspase-3, MDM2, and p53 determined by western blot.  $\beta$ -actin levels served as loading controls.

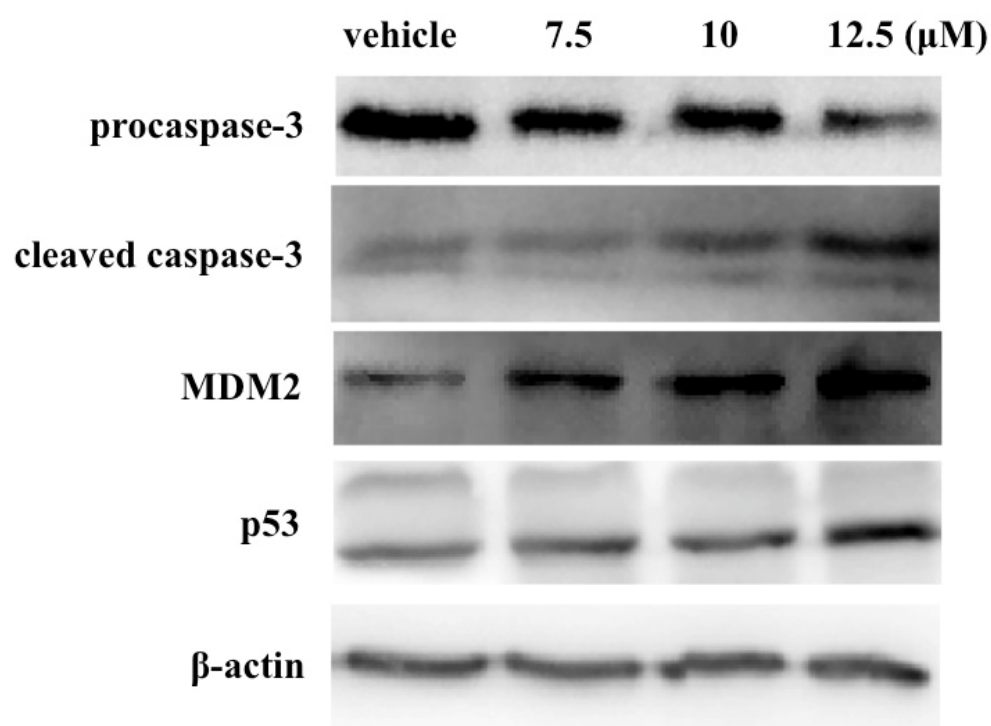
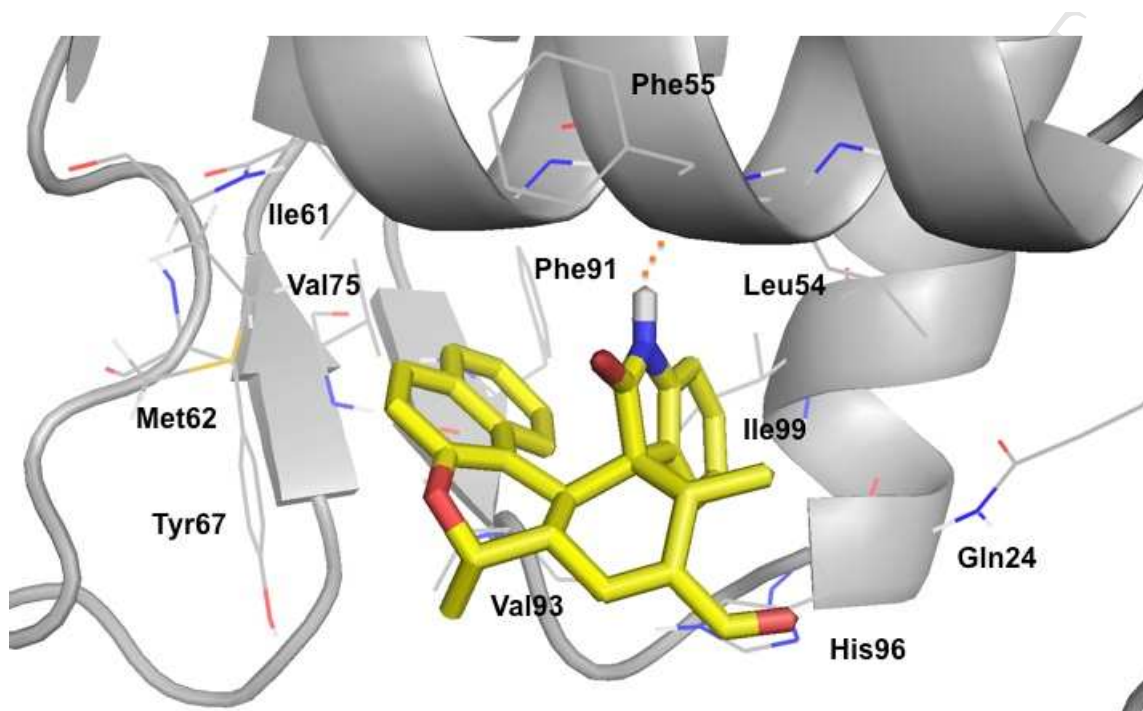


Figure 8. Predicted binding configuration of compound **10i** (non-polar hydrogen atoms undisplayed) into the p53-binding site on MDM2 (4OAS.pdb[21]).



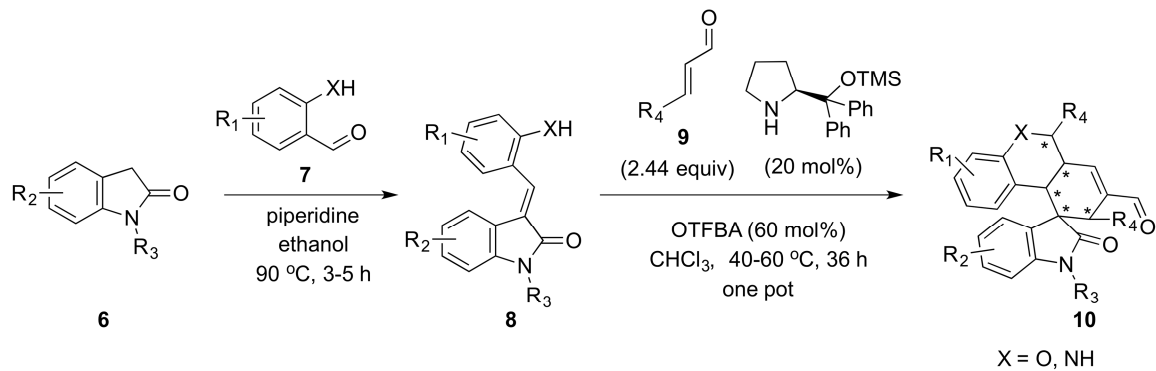
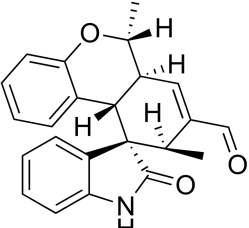
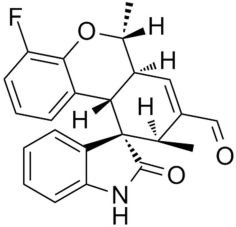
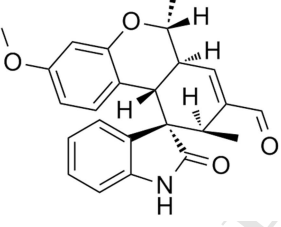
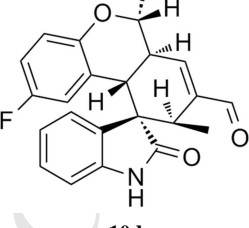
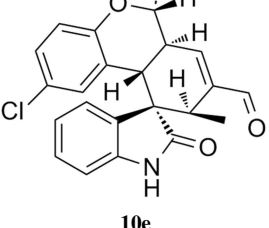
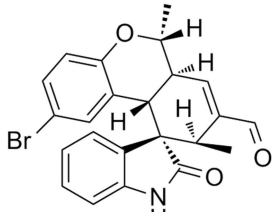
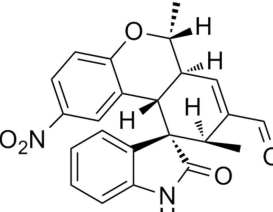
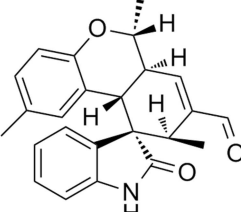
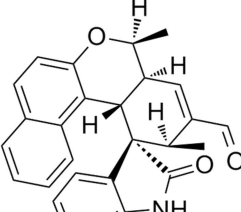
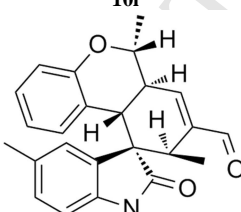
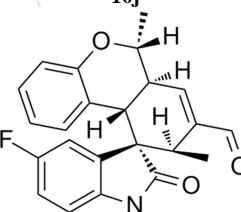
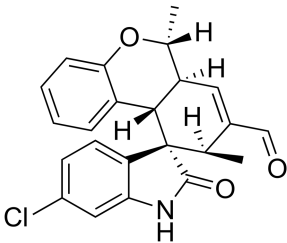
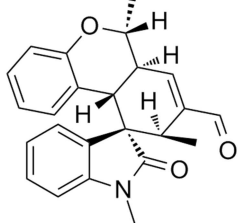
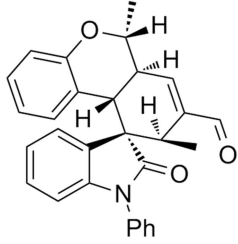
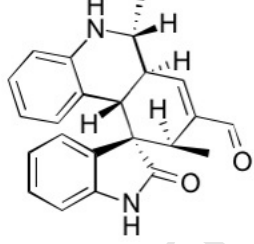
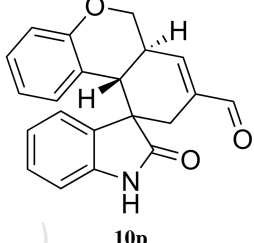
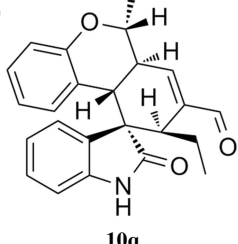
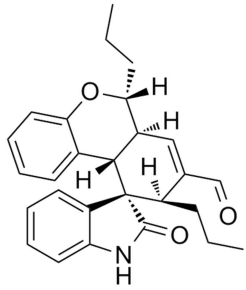
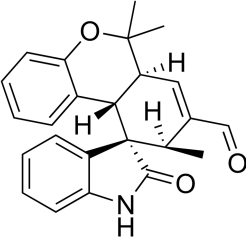
Scheme 1. Synthetic route to spirooxindole derivatives **10a-s**.

Table 1. Antiproliferative activities of the compounds **10a-s** against A2780s and A2780T cells *in vitro*.

Entry	Structure	Percent Inhibition at 30 $\mu$ M or IC <sub>50</sub> ( $\mu$ M) <sup>a</sup>	
		A2870s	A2870T
1	 <p><b>10a</b></p>	23.5%	17.3%
2	 <p><b>10b</b></p>	22.2%	5.7%
3	 <p><b>10c</b></p>	9.3%	3.9%
4	 <p><b>10d</b></p>	22.7%	2.6%
5	 <p><b>10e</b></p>	16.5%	5.8%

6	 <b>10f</b>	35.9%	2.3%
7	 <b>10g</b>	25.2%	0.2%
8	 <b>10h</b>	28.2%	10.4%
9	 <b>10i</b>	<b>7.9</b>	23.4
10	 <b>10j</b>	12.8%	7.1%
11	 <b>10k</b>	14.5%	4.4%

12	 <b>10l</b>	<b>19.7</b>	13.1%
13	 <b>10m</b>	26.3%	4.5%
14	 <b>10n</b>	<b>18.9</b>	40.6%
15	 <b>10o</b>	47.2%	15.2%
16	 <b>10p</b>	<b>21.6</b>	25.0%
17	 <b>10q</b>	34.1%	9.0%

18	 <b>10r</b>	<b>25.7</b>	<b>33.1%</b>
19	 <b>10s</b>	<b>14.4%</b>	<b>3.8%</b>
20	<b>cisplatin</b>	<b>20.9</b>	<b>27.3</b>

<sup>a</sup>Values were average of three determinations and deviation from the average is less than 5% of the average value.

Table 2. Antiproliferative activities of the compounds **10a-s** against H1299, BGC823, CT26, HCT116, A549, MCF7, and H1975 cells *in vitro*.

Entry	Compounds	IC <sub>50</sub> (μM) <sup>a</sup>						
		H1299	BGC823	CT26	HCT116	A549	MCF7	H1975
1	<b>10a</b>	> 30	> 30	> 30	> 30	> 30	> 30	> 30
2	<b>10b</b>	> 30	> 30	> 30	> 30	> 30	> 30	> 30
3	<b>10c</b>	> 30	> 30	> 30	> 30	> 30	> 30	> 30
4	<b>10d</b>	> 30	> 30	> 30	> 30	> 30	> 30	> 30
5	<b>10e</b>	> 30	> 30	> 30	> 30	> 30	> 30	> 30
6	<b>10f</b>	> 30	> 30	> 30	> 30	> 30	> 30	> 30
7	<b>10g</b>	> 30	> 30	> 30	> 30	> 30	> 30	> 30
8	<b>10h</b>	> 30	> 30	> 30	> 30	> 30	> 30	> 30
9	<b>10i</b>	> 30	> 30	9.5	8.6	18.3	16.2	13.7
10	<b>10j</b>	> 30	> 30	> 30	> 30	> 30	> 30	> 30
11	<b>10k</b>	> 30	> 30	> 30	> 30	> 30	> 30	> 30
12	<b>10l</b>	> 30	> 30	> 30	> 30	> 30	> 30	> 30
13	<b>10m</b>	> 30	> 30	> 30	> 30	> 30	> 30	> 30
14	<b>10n</b>	30	25.7	> 30	> 30	> 30	> 30	> 30
15	<b>10o</b>	> 30	> 30	> 30	> 30	> 30	> 30	> 30
16	<b>10p</b>	> 30	> 30	27.1	25.8	> 30	> 30	> 30
17	<b>10q</b>	> 30	> 30	> 30	> 30	> 30	> 30	> 30
18	<b>10r</b>	> 30	> 30	> 30	> 30	> 30	> 30	> 30
19	<b>10s</b>	> 30	> 30	> 30	> 30	> 30	> 30	> 30
20	<b>cisplatin</b>	8.9	19.8	23.7	17.4	15.6	7.8	9.7

<sup>a</sup>Values were average of three determinations and deviation from the average is less than 5% of the average value.



**Highlights:**

1. Nineteen novel polycyclic spiro-fused carbocyclooxindoles were investigated.
2. Compound **10i** displayed inhibitory activities against seven cancer cell lines.
3. **10i** arrested cell cycle in G1 phase and induced apoptosis.
4. **10i** enhanced the protein levels of cleaved caspase-3, p53, and MDM2.
5. Docking studies showed **10i** might block the MDM2-p53 interactions.